EVALUATION OF TORSO STABILITY USING THE BASIN OF STABILITY CHAIR

by

Walter Dalton Fox

A thesis submitted to the

Faculty of the Graduate School

of

Western Carolina University

in partial fulfillment

of the requirements for the degree of

Master of Science in Technology

Martin Tanaka, Ph.D., Chair

Paul Yanik, Ph.D.

James Zhang, Ph.D.

Kimmel School Department of Engineering and Technology

Western Carolina University

December 2013

ACKNOWLEDGEMENTS

I would like to thank my thesis director, Dr. Martin Tanaka, and my committee members, Dr. Paul Yanik and Dr. James Zhang. In addition, I would like to express my sincere gratitude to the Western Carolina University Graduate School for awarding the Faculty Research and Creative Activities Grant and the Kimmel School's Center for Rapid Product Development for awarding the Center for Advanced Technology Grant to Dr. Tanaka. Funds from these grants were used to purchase the materials used to build the device described in this thesis. Finally, I would like to thank Mr. Monty Graham for providing assistance with our machining facilities, and Ms. Allison Krauss for helping in the procurement of the materials needed to complete this research.

I would also like to acknowledge the passing of my father, Peter Dalton Fox, who did not get to see the completion of this research. He proudly supported me throughout my undergraduate degree and was always interested in the facilities at The Kimmel School. I am glad that I was finally able to use them to build and contribute a novel piece of research with his support.

TABLE OF CONTENTS

LIST OF TABLES

LIST OF FIGURES

ABSTRACT

EVALUATION OF TORSO STABILITY USING THE BASIN OF STABILITY CHAIR

Walter Dalton Fox, M.S.T.

Western Carolina University (November 2013)

Director: Dr. Martin Tanaka

Low back pain (LBP) is a costly problem in modern health care that affects up to 80% of the population at some point in life. The link between low back and torso instability or spinal motion has not been clearly defined. Past studies evaluating torso dynamics have employed the use of *unstable seating apparatuses* to analyze various aspects of human torso stability. Traditionally, these devices measure *Kinematic Variability* (KV). However, previous devices had design limitations making them unable to measure dynamic stability parameters such as the *Basin of Stability* (BoS). In this research project an innovative new device for measuring unstable seating was designed, constructed, and performance tested.

The new device, the BoS Chair, presented several key challenges and required the custom fabrication of each major component utilizing CAD software and CNC machinery. A new seating arrangement was devised using a kneeling chair configuration to isolate the upper torso. The new seating configuration implemented a high deflection angle joint allowing the chair to tilt farther than previous devices enabling the calculation of the basin of stability. The design also required the ability to adjust restorative torque,

known simply as the difficulty level. These features required safety measures and a sturdy safety frame to accompany the device.

Testing of the new BoS chair required the formulation of Threshold of Stability (ToS) and Basin of Stability test procedures. The ToS procedure tested participants through a series of increasing difficulties until failure was detected. The point of failure marked the threshold of the participant. Using the ToS information, a preliminary BoS procedure was conducted to record temporal movement parameters using a gyroscopic sensor. Tests were conducted with six male and six female participants.

ToS trials were statistically compared and analyzed, revealing that height and weight had a significant confounding effect on the results. The effect was successfully remedied through normalization. It showed that the BoS chair could be used to study the torso balance control of participants regardless of their size. The stability graphs and stabilograms generated from the preliminary BoS data indicated that the recording device and trial methods were sufficient. These initial Basin of Stability tests will form the foundation for the development of future BoS testing protocols.

The BoS chair is as a durable and flexible tool for measuring torso stability that was designed to detect Lagrangian Coherent structures in a novel way. The preliminary BoS data collected in this research will be useful for future Basin of Stability research and provide preliminary data for grant proposals. With the device constructed and baseline data available for human subjects (i.e. controls), we are now prepared for future projects that measure torso stability in patient populations to improve our understanding of this condition and its effect on low back pain.

CHAPTER 1: INTRODUCTION

1.1 Low back pain

Low back pain (LBP) is a costly problem in modern health care that affects up to 80% of the population at some point in life (Lee 2011, Vaughn 1999). LBP can be classified as any back pain experienced between the ribs and the top of the leg, and it is a major occupational impairment around the world (Frank 1996). Few research studies have examined the actual relationship between spinal motion and low back pain (Dickey 2000). Most LBP cases are found to be mechanical in origin, meaning the pain is aggravated by movement (Bogduk, Twomey 1991). However, existing studies have also failed to observe differences in spinal motion between LBP sufferers and normal subjects (Marras 94). Ruhe (2011) utilized a numeric rating scale to measure perceived pain intensity in LBP patients. It was found that pain levels that scored above 9 out of 10 are not commonly encountered due to the severity usually resulting in immediate medical attention. Regardless, Ruhe was able to find a linear relationship between pain intensity and postural sway, though this still does not define the link between LBP and stability.

1.2 Torso stability

Torso stability is a dynamic measure of spinal kinematics that can be hindered by low back pain. It is the duty of the spine, paraspinal ligaments, core musculature, and neuromuscular control system to maintain upright posture (Tanaka 2009). It is the concern of several researchers (Cholewicki, 2003; Panjabi, 2003; Granata, 2004; Tanaka, 2007) that loss of spinal stability can strain spinal tissues which can lead to low back

pain. Though LBP sufferers do not typically exhibit obvious abnormalities through static motion conditions, spine abnormalities can be revealed through dynamic spinal motion (Bogduk, Twomey 1991; Lee 2011). The stable control of human upright posture has been compared to a continuous process of stabilizing a multilink inverted pendulum (Maurer and Peterka 2005; Blaszczyk 2008). In 2007, Tanaka reported a growth in spinal stability research. His search on PubMed yielded 2611 publications dating back to 1963. As of this writing the number has risen to 3940, including 233 published this year.

1.3 How low back pain affects torso stability

In low back pain conditions, patients might not be able to utilize all of their degrees of freedom (DOF) to stabilize the body's center of mass (Tajali 2011). Degrees of freedom are regarded as any joints or combination of joints in the body controlled through the central nervous system (CNS). LBP can cause inhibitions within the degrees of freedom and therefore alter the kinematic chain controlling the body's center of mass (Tajali 2011). To capture these spinal dynamics, researchers in the past have utilized optical tracking via skin markers, electromagnetic trackers, and portable internal sensors (Lee 2011). A similar test (Spyridonis 2010) used pressure mapping in conjunction with 3D pain drawings. 3D pain drawings are used to graphically record pain on a 2D human diagram (Ransford 1976). Much like the basin of stability research, this was an exploratory study to investigate new methods for back pain assessment. This helped to shed light on the correlation between postural habits and resulting low back pain.

In a test to detect impaired postural control and delayed muscle response times, patients with chronic low back pain exhibited poorer postural control and longer trunk

muscle response times than healthy volunteers (Radebold & Cholewicki 2001). LBP is also associated with significant decreases in range of motion and velocities of the spinal and pelvic motion (Lee 2011). These reactions may be rooted from LBP patients' efforts to reduce pain by restricting movements due to the presence of LBP or fear-avoidance behavior affiliated with LBP (Vlaeyen, Linton 2000). The authors show that there is a strong relationship between segmental spinal range of motion and level of pain experienced, and these findings allegedly isolated the cause to the lumbar spine.

1.4 Current methods to measure torso stability

Torso stability is divided into two factors; static stability and dynamic stability. Static stability defines the potential to move. In a static system, restorative forces must overcome destabilizing forces (Panjabi, 1992). In a statically stable system, destabilizing forces that tend to move the torso away from equilibrium are less than the restorative forces stabilizing the torso. Dynamic stability evaluates systems in motion. Ruhe's study on postural sway (2011) is an example of dynamic stability. Dynamic stability takes into account the system velocity and momentum in the determination of torso stability (Tanaka 2009).

Kinematic Variability (KV) is among the parameters that detect motion in a system, but do not indicate stability. Kinematic variability is best known for its use in analyzing center of pressure (CoP) or center of mass (CoM) data (Blaszczyk 2008; Tajali 2011; Ruhe 2011). The center of pressure is the location on the soles of the feet where the entire body mass could be concentrated to one spot (Ruhe 2011). The center of pressure method was utilized by Radebold and Cholewicki (2000). Radebold and Cholewicki

tested torso stability using a commonly available stability ball. The apparatus consisted of a chair mounted upon a hemispherical ball. The unstable surface influenced motion through the lumbar spine, and concentrated pressure on a central point. This unstable seat apparatus is used in numerous subsequent studies.

ToS is defined as "the maximum task difficulty in which stability can be maintained" (Tanaka 2009). Tanaka's evaluation of the threshold of stability called for the alteration of task difficulty during trials. Through task difficulty manipulation, kinematic variability increased while the basin of stability (BoS) simultaneously decreased. The "wobble chair" used for this test had springs to control the restorative moment across a low friction ball joint. When the springs were moved closer to the center, the restorative moment diminished as the task difficulty increased. Trials were carried out at different spring settings so that the ToS could be evaluated. The study resulted in a foundation for further study.

1.5 Basin of Stability

Basin of stability research begins with the basin of attraction. In a study on passive dynamic walking the basin of attraction was explored through pendulum motion (McGeer 1988). McGeer studied the possibilities of designing a way for robots to walk without exerting energy. As a pendulum, or leg, swings it is attracted to the lowest point of the swing, and this potential energy may be exploited. The basin of attraction contributes to research such as cyclic motion and passive walking robots as it can reveal ways to save energy (Liu 2007). The basin of stability is similar to a basin of attraction in

torso stability research (Figure 1.1). The basin of stability is the region in state space where stable behavior occurs (Tanaka 2009).

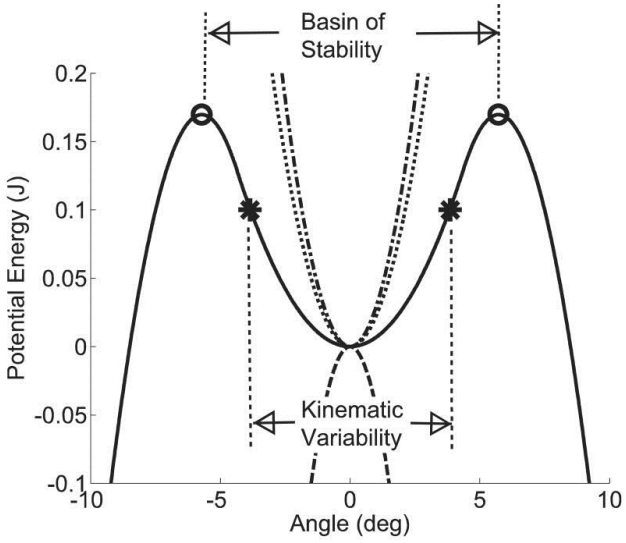

Figure 1.1: KV plot with Basin of Stability

1.6 Kneeling chairs

The unstable seat apparatus and wobble chair both used similar seating platforms which resembled that of an office chair configuration. An alternative seating configuration is the Balans chair (Figure 1.2) which has existing since the 1970's and could offer an ergonomic advantage. "The chair designed accurately is able to make muscles relaxed, reduce physical expending, avoid tiredness, and is helpful to keep the body steady for intensive work" (Jiefeng 2009). A kneeling orientation would mimic a standing posture to keep the spine in a natural configuration (Jiefeng 2009). The forward tilt serves to incline the body forward to retain natural curvature of the spine that would reduce stress on the lumbar spine. The use of a Balans chair is also sought to enhance aspects of the center of pressure.

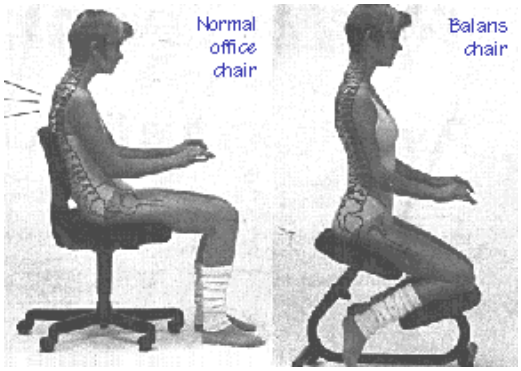

Figure 1.2: Comparison of a normal chair versus a Balans Chair

Previous studies in the field of torso stability have utilized devices known as "unstable seating apparatuses" to analyze torso dynamics. These devices were either not easily adjustable for different difficulty levels (Radebold & Cholewicki 2001) or they were unable to attain large deflection angles (Granata 2004) needed to detect the basin of stability. The objective of this thesis research is to design, build and test a new device, the BoS chair, which is continuously adjustable and capable of the large deflection angles needed to detect the basin of stability.

CHAPTER 2: DESIGN & CONSTRUCTION

A key element of this thesis project was the design and construction of the BoS chair. The BoS chair is the latest in a series of devices in the line of *wobble chairs*, or *unstable seating apparatuses*. This new design needed to include additional capabilities that allowed for the measurement of the Basin of Stability. Design requirements include the ability to achieve high deflection angles, rigid attachment of the top plate to the bottom structure through a pivot joint, adjustability of restorative torque, and a safety frame. The design needed to be robust and simple enough to last through a dozen trials. Fabrication work was constrained to that which could be performed with the facilities available to the researchers.

2.1 Design concepts

The BoS chair design included longer springs, and a more robust ball joint. A new seating system was devised to separate from the lower mechanism so it could be attached to varying designs. A rough draft of the seat and lower mechanism as a whole was then modeled in Pro/ENGINEER to better understand the geometries. As the model took shape, essential parts were chosen that could be applied to existing and future designs. The physical parts obtained for the conceptual stage were four springs and a 4” ball joint which were considered robust and common enough to base the entire chair design on. The items were then modeled in Pro/ENGINEER to be incorporated in all BoS models and drawings. They could also be adapted to numerous potential design changes. The 3D model of this conceptual model is shown in Figure 2.1.

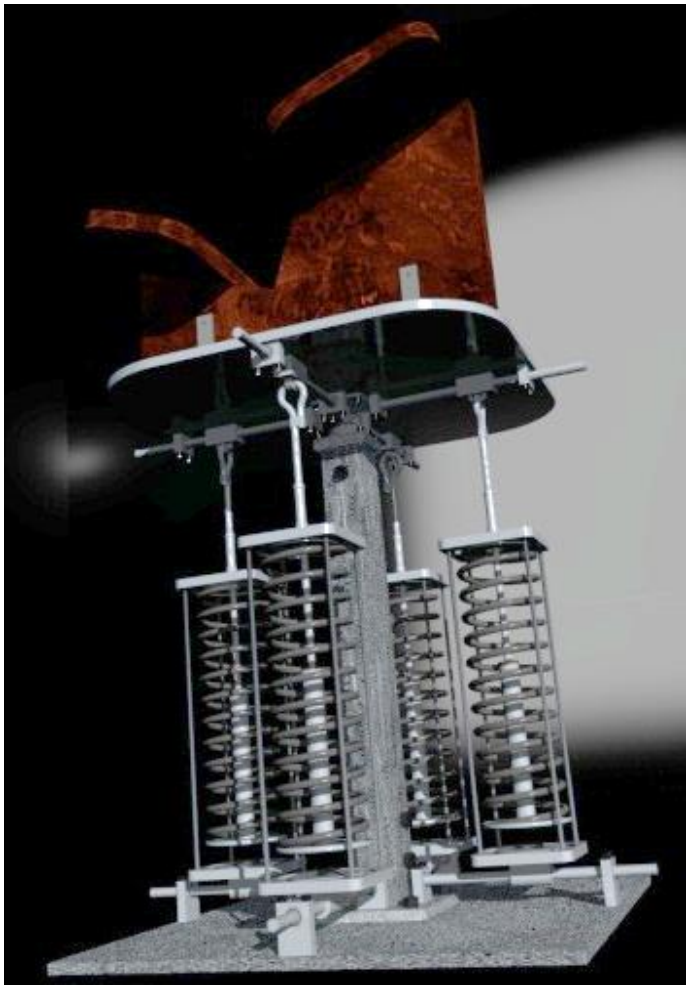

Figure 2.1: 3D CAD Model of design concept created using Pro/Engineer.

2.1.1 Alternative design concepts

Alternative designs for the BoS chair were also evaluated. However, the alternatives were found to be too complex, expensive, or even too risky to build in the first iteration. This section explores different geometric designs, as well as different power-assisted methods. When a basic draft for the first design was finished, the other options were explored for reassurance that the best design had been chosen. All concepts featured the same seating device.

Power-assisted methods were considered and sought after for their precision and power. A second geometric design was created to be compatible with various methods of power assistance. Hydraulics, pneumatics and electric motors were all considered for application in the new design. A chair mechanism with two pivot points instead of a single ball joint was considered. With 2 axes of motion, each axle could be controlled by linear hydraulics or pneumatics, or by rotational electric motors. The result of this concept yielded a device that resembled a gimbal or a gyroscope as shown in Figure 2.2.

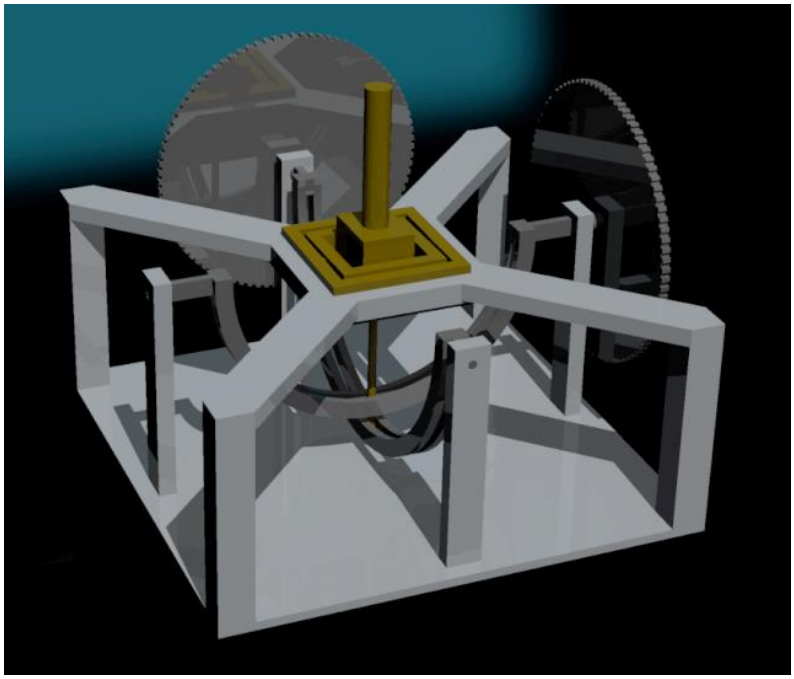

Figure 2.2: 3D representation of gimbal design.

A gimbal joint was used to hold the upper chair in place. The joint was similar to a U-joint that allowed the center to move with the outer section remaining stationary. The advantage of the gimbal joint was to gain one continuous “down rod” arm from the chair to the control arms below. The gimbal also offered a more compact design to keep the chair lower to the ground. The motion control arms are the two curved bars spanning

across the device perpendicular to one another. The control arms are the two axes used to control motion of the chair when connected to a power assisted device. The down rod was inserted into channels in the control arms where it could slide along an axis, or push against the axis, as shown in Figure 2.3, right.

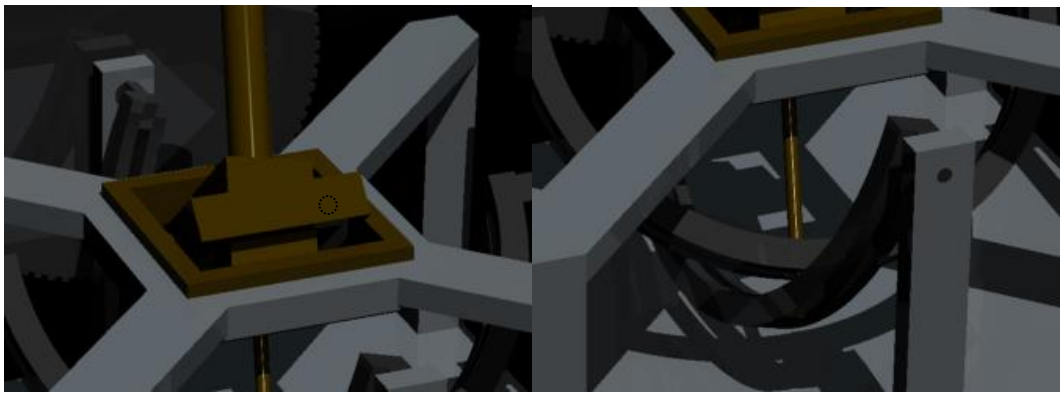

Figure 2.3: Gimbal joint in motion (left), the down rod engaging control arms (right).

As the control arm moves as a result of feedback from a participant attempting to balance on the chair above, the control arms follow along. The control arm on the x-axis follows left and right. The control arm on the y-axis follows forward and aft. The arms are curved at different diameters so they do not interfere with one-another. The control arms were connected to the frame with needle bearings so they could swing freely. Located on one side of each arm was a through-hole that allowed for means to rigidly connect to a power assisted device to control or provide restorative torque to the chair.

2.1.2 Power assisted concepts and actuators

Pneumatic actuators were the first technology considered to provide power assisted motion control to the chair. Two to four actuators would be connected to the outputs of the control arms of the gimbal design. The cylinders were attached to the end

of a lever to push and pull as the chair moved as shown in Figure 2.4. A pneumatic control system connected through hoses was to be implemented to govern the actuators and provide specific actuator resistances at different difficulties in the testing phases.

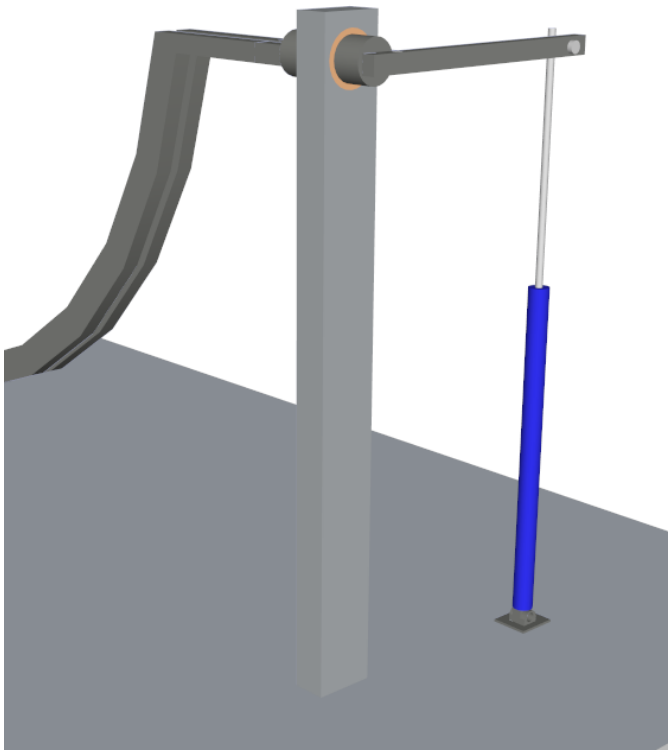

Figure 2.4: Adaptation used to connect an actuator (blue) to the control arm

Pneumatic actuators were rejected due to the use of gas pressure to control motion. A quick test with a pneumatic strut kept in the lab revealed that pneumatics may be too imprecise when trying to control or dampen motion because the gases inside are compressible. The gases inside the strut were thus unpredictable, and would likely be too difficult to maintain calibration with the pneumatic control system. Hydraulic cylinders were a viable substitute, and could be applied in the same manner as the pneumatic actuators. Despite the advantage of fluid dynamics over pneumatics, hydraulics was also

rejected. Hydraulics could not be utilized due to slow response times and cumbersome equipment.

Electric motors were considered for their precision and ease of use. Each of the two control arms was to be designated to be controlled by one stepper motor. The motors were to be connected to the arms with a gear set of a specific ratio. In theory, the motors would have been able to control the motion of the chair in lieu of springs or other actuators. Using a control system, the power, and hence, the resistance of each motor could have been adjusted simultaneously. Unfortunately, the cost of two motors of adequate power with a control system, plus the time needed to install and calibrate them was beyond the scope of the project.

All power-assisted designs would require a complex control system that would have to be assembled and calibrated. The only advantage was the ability to throttle the difficulty at the turn of a dial. It was ultimately decided that power-assistance fell outside the scope of the project due to cost and the time required to develop the system.

2.1.3 Final design

The original concept was revisited and chosen for its simplicity. Using the models for the springs and ball joint, a new assembly model was designed in Pro/ENGINEER. The new model was built more concisely to fully realize the appearance and geometries of the finished BoS chair. The assembly was given articulation to simulate motion of the chair with all four springs attached. The model was not used directly for fabrication, nor converted to CNC language. The geometries for most parts were simple enough to be defined manually, resulting in fewer steps taken to complete

the device. The design of the BoS chair was divided into ten major sections, as shown in Figure 2.5.

1. Chair
2. Chair slider
3. Pivot joint
4. Pivot plate
5. Spring enclosure
6. Base
7. Spring traverse
8. Control cables
9. Safety frame
10. Adjustment tool

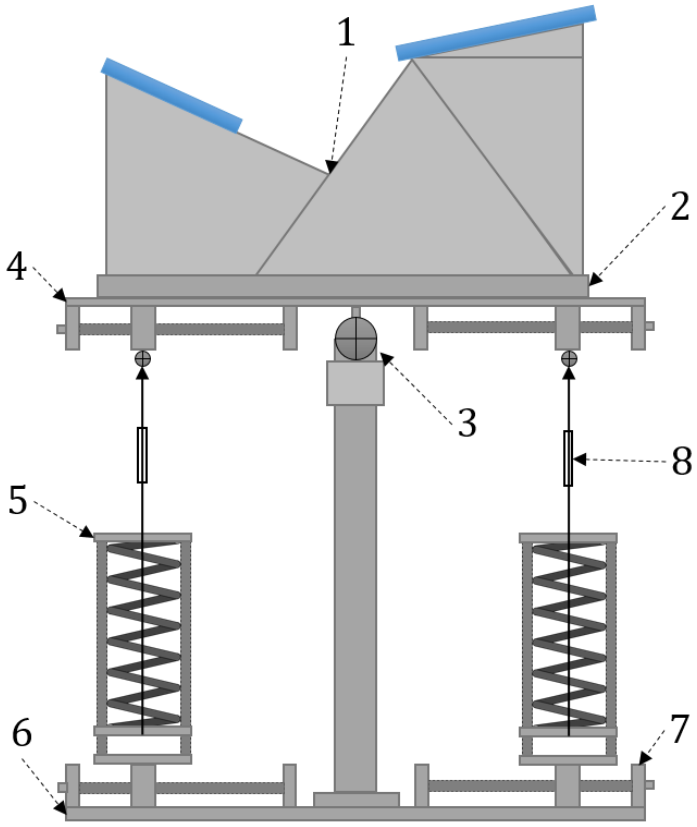

Figure 2.5: Cross-sectional diagram of the basic components of the BoS chair.

2.2 Detailed design and fabrication

This section serves to describe the individual parts that make up the BoS testing platform. The BoS testing platform is comprised of the BoS chair, safety frame, and recording devices.

2.2.1 Manufacturing equipment utilized

Computer Numerical Control (CNC) machining practices were employed to yield precise geometries and accurate feature locations on all parts. OneCNC provided the means needed to create programs and templates for each process. No complex geometries are featured in the design of the BoS chair. Therefore, there was no need to import CAD files and convert them into CNC code. Thus it was faster to manually create simple CNC code for each part and make minor adjustments as needed.

Milling, drilling, and hole-tapping were all performed on a HAAS VF-1 Mill. The mill allowed for rapid removal of material with clean finishes. Small parts such as retainers and plates were sometimes made in series across one piece of stock material and then cut apart. This method yielded the mass production of identical parts used throughout the chair, eliminating the setup times needed to make numerous parts individually. Larger parts in the assembly required more elaborate CNC code.

The HAAS Lathe was used for some manual operations necessary to complete the device. The tolerances applied to the dimensions throughout the device were relatively low. The basic precision gained through use of CNC was more than sufficient to ensure that all parts and mechanisms performed as expected.

2.2.2 Materials

The raw materials that compose the chair were chosen to be wood, aluminum, and steel. These materials were designated to specific locations and parts on the device based on weight and machinability. The intention was to utilize heavier materials in lower sections of the device to enhance stability and durability. All parts above the pivot point of the chair were built from either 6061 aluminum or plywood to reduce the weight, and

thus, the moment of inertia of all upper components. Other materials include foam and plastics to enhance function and safety.

Various products were used in conjunction with the raw materials to create the moving and functioning parts of the chair. Four springs were tested for function and incorporated into the spring enclosures. ACME threaded rod was used to create the traversing mechanism for the spring enclosures. This threaded rod was resistant to lateral load, and was ideal for quantifying measurements. A flange-mount ball transfer used in conveyor systems was repurposed for a load bearing pivot joint for the chair. 0.5" needle bearings were used in all rotating connections within the spring traverse mechanism. Needle bearings were chosen for their lateral load tolerances and small profile over ball bearings. Finally, 5/16-18 socket cap screws were acquired in various lengths to be used to fasten all components within the design. The use of one common screw type simplified the design and offered sufficient durability.

2.2.3 Chair design and fabrication

The chair was the first part of the BoS chair to be built. The chair achieves an upright seated position similar to the Balans chair design. It was intended to be compact, rigid, light weight, and to have no moving parts. Because the chair was the highest component above the pivot point, it was important to reduce weight and thus, the chair's moment about the pivot point. Figure 2.6 shows the chair in relation to the full design.

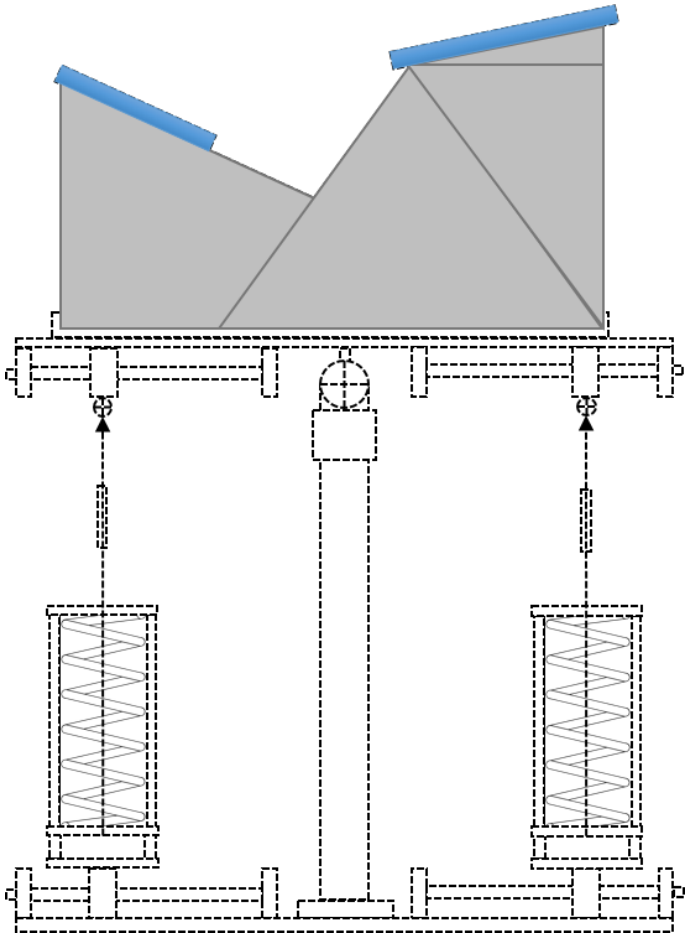

Figure 2.6: Isolated view of the kneeling chair in relation to the assembly

The geometry of the seat was critical to the behavior and ergonomics of the BoS chair. The seat needed to accommodate various sizes of adult participants in a kneeling position while being as low as possible to the base plate. A lower profile was needed to reduce the moment about the pivot point and decrease the workload of the control springs. To determine the optimal seating geometry, a jig was made to mimic the seating configuration of a typical kneeling chair as shown in Figure 2.7. The jig was made of 2x4's, consisting of a simple frame with movable panels that acted as the seating planes of a Balans chair. The movable panels were held in place with hinges and clamps so they could be moved forward, aft, up and down. Various configurations resulted in different

angles and elevations of the seating planes. Ultimately, the jig was used to find the lowest comfortable configuration to seat a tall male (74”). The measurements resulted in a chair no taller than 17” at its highest point, with a center of mass approximately 12” above the pivot point. These dimensions were recorded and applied to the chair drawing.

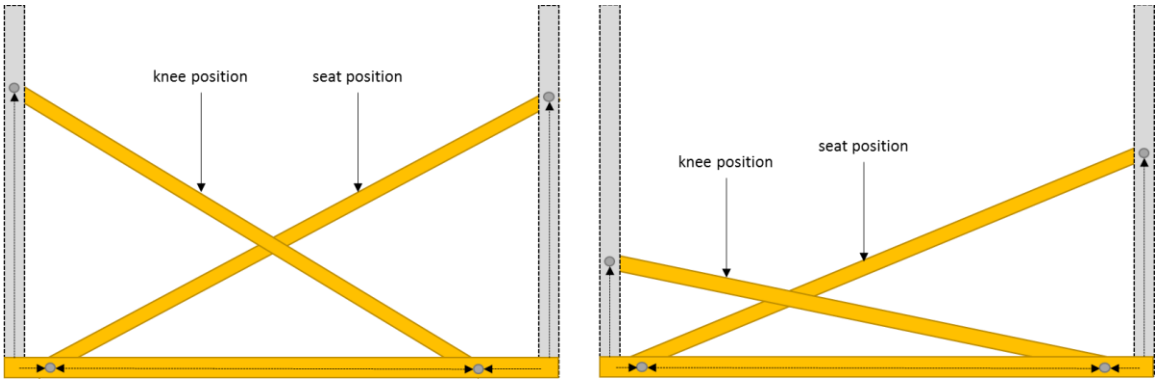

Figure 2.7: Comparison of two different possible configurations of the dimension device

Using the dimensions obtained, a two dimensional template was drawn onto a 0.75” thick sheet of plywood to create the upright base of the chair as shown in Figure 2.8. The plywood was then cut and shaped to the form of the template. The rear seat and knee rest were also cut on the band saw. The rear seat and knee rest were fastened to the upright base using wood screws and lightweight shelf brackets for durability. Initial observations revealed that the seat had a tendency to contort under load, which led to the fabrication of an identical upright section. This was fastened to the original, doubling the thickness. The completed chair weighed approximately 12 lbs., 5 to 10 percent of the weight of a typical young adult participant (estimated at 120 to 230 lbs.). The chair was also easy to work with and resistant to structural fatigue imposed by participant weight. Padding was later added to cover the abrasive wood, making the chair more comfortable.

Figure 2.8: Basic wood components of kneeling chair (left), incomplete kneeling chair being tested (right)

2.2.4 Chair slider design and fabrication

A slider was designed to allow the chair to slide forward and aft along the pivot plate. The adjustment allowed the chair to be moved in the sagittal plane so that the center of pressure could be positioned over the pivot point. The design needed to be simple and robust to ensure a firm connection to the chair capable of enduring hours of testing. The design consisted of four elongated bars with an "L" shaped cross-section. The "L" shapes interlocked, forming a T-slot for the chair to rest in as seen in Figure 2.9.

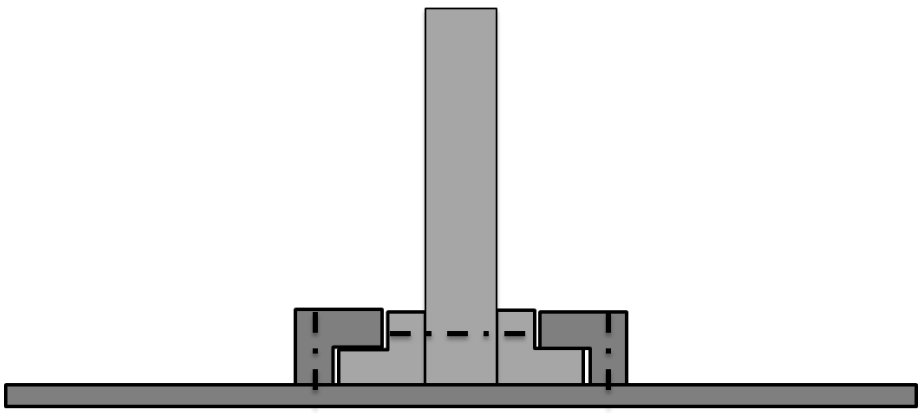

Figure 2.9: Cross-sectional view of the interlocking shapes

The four pieces of extruded aluminum were milled using very simple linear operations. Holes were then drilled for attachment points along the length of the bars. The first two bars were made to be identical and fastened to the sides of the chair with two through-bolts. The second pair was bolted to the pivot plate. The chair was then inserted into the T-slot and slid into place. The slider feature was finalized by adding set screws used to lock the chair in place.

2.2.5 Pivot joint design and fabrication

A pivot joint was needed to allow motion of the upper components of the BoS chair. The joint was to be located between the base structure and the pivot plate. A robust joint was required that could achieve approximately 70° of tilt in all directions. U-joints were considered, but avoided because they are not typically designed to support a compressive load. Flange-mount ball transfers, shown in Figure 2.10, provided the load bearing pivot body needed. However, the ball transfer required modification in order to be utilized as a “ball and socket” joint.

Figure 2.10: General illustration of a flange-mount ball transfer. Retrieved from: http://www.mcmaster.com/#standard-ball-transfers-for-conveyors/=mnq0yi

To remedy the lack of attachment on the top side of the joint, a 0.5” diameter steel rod was cut to 1” and TIG welded to the ball. A 4” square steel plate with a center hole for the steel rod was then welded in place. A temporary jig simultaneously held the ball

transfer and steel plate together ensure all axes were aligned for welding. After welding, the jig was removed to reveal a working “ball and socket” joint with suitable connections for the base and pivot plate. The final ball joint highlighted in Figure 2.11 was capable of a maximum tilt of 75° in all directions while maintaining smooth and quiet motion under load.

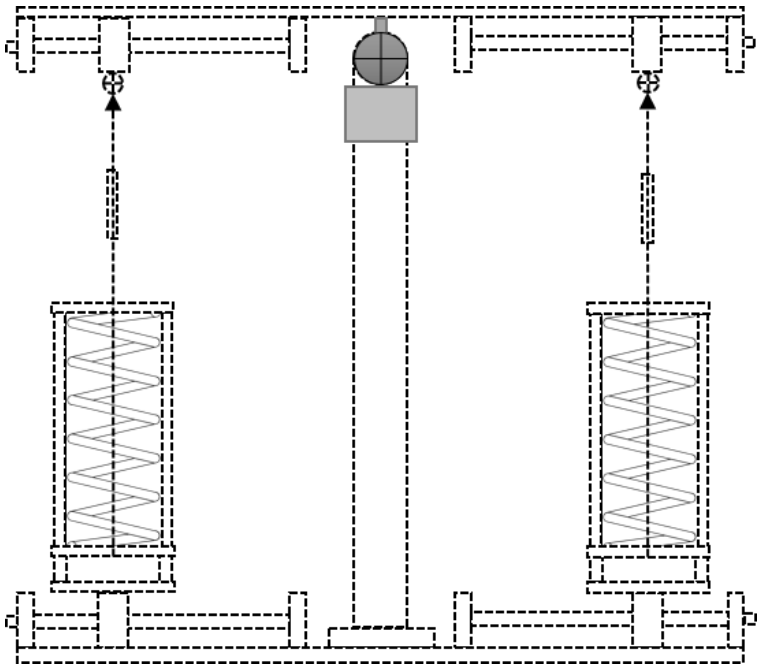

Figure 2.11: Isolated view of the ball joint.

2.2.6 Pivot plate design and fabrication

The pivot plate was designed as the central connection hub for all moving attachments in the top portion of the BoS chair shown in Figure 2.12. The pivot plate provided attachment locations for the seat with slider, the pivot joint, and the four variable connections to the control springs. The plate was also intended to act as a barrier and foot rest to keep participant appendages clear of the working mechanisms below.

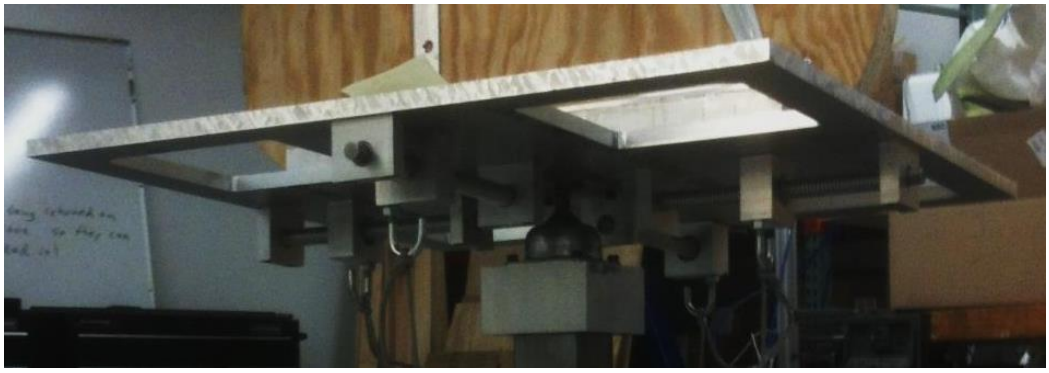

Figure 2.12: View of the ball joint installed between the adapter and pivot plate.

The plate was formed from a 2’ by 2’ by 0.5” thick 6061 aluminum plate. 6061 aluminum alloy was chosen for its light weight and machinability. The oversized plate needed to be custom mounted in a HAAS VF-1 End Mill for further processes. All necessary holes were drilled and tapped. The holes were necessary for mounting the spring traverse mechanism, chair slider, and ball joint connection with socket cap screws. Sections of the plate were cut away to reduce weight (and moment about the pivot point) wherever it could be spared. The corners were removed to prevent them from impacting the safety frame covers.

2.2.7 Spring enclosure design, fabrication and testing

Four spring enclosures were designed and built to house the control springs. The enclosures were necessary to mount the springs rigidly to the chair and to safely contain the springs in case of catastrophic failure. The spring used is a compression spring, rated at 42 pounds per inch, a spring rate similar to that of the original wobble chair springs. The enclosure was designed to compress the spring making it function similarly to an extension spring. Compression springs were used instead of extension springs because

there are many more choices for compression springs than extension springs, and one with appropriate characteristics could be found. Figure 2.13 defines the locations of spring enclosures in reference to the full design.

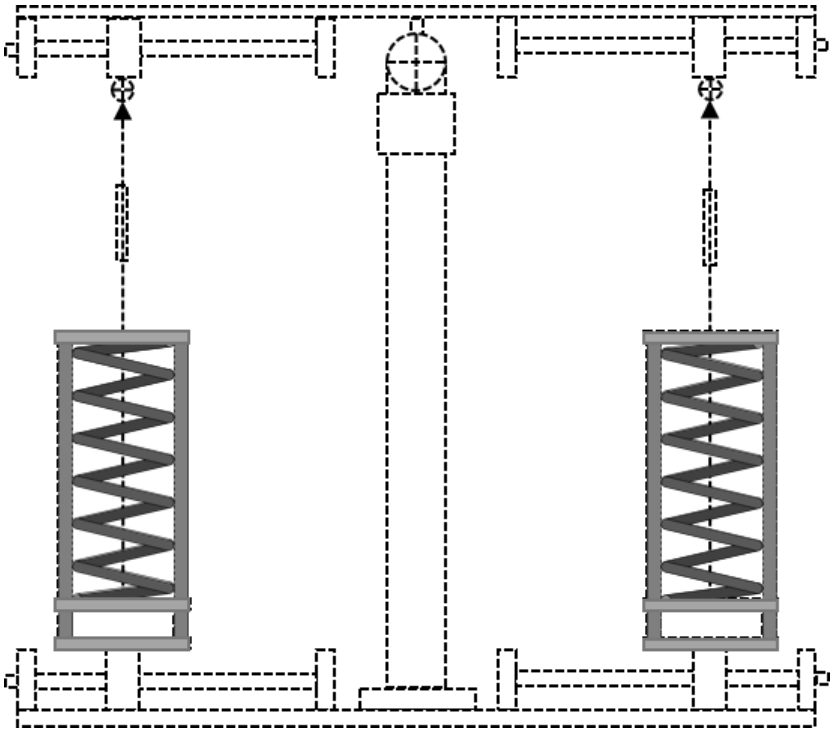

Figure 2.13: Isolated view of spring enclosures.

Steel cables were chosen to connect the springs to the chair. Cables offer a flexible connection that is easy to install, modify and adjust. Cables can only be used to pull or suspend an object, further supporting the compression-only design. If the chair were to move in a direction that did not apply an upward force on a particular spring, the cable would slacken. A slackened cable on one spring would result in uncompromised actuation of a spring on the opposite side of the chair. To make the cables compress the

springs, they were connected through to the bottom of the spring, to apply upward forces from the bottom shown in Figure 2.14.

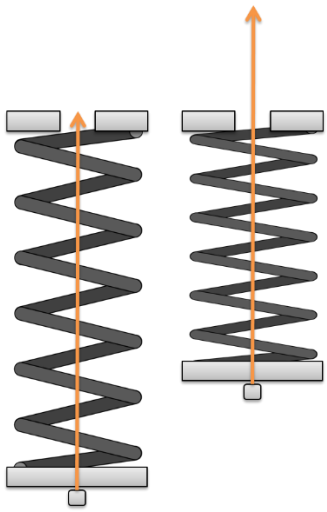

Figure 2.14: Drawing of a spring at rest (left), and a spring engaged (right).

Twelve plates of aluminum were cut from stock into 4” x 4” squares to form the template of the spring enclosures. A two-dimensional palette was made in OneCNC with the pattern for three different plate designs. The first plate had a circle congruent with the diameter of the spring. The circle was cut with a ball mill half way through the plate to make a cupped seat for the spring to rest. The rounded groove allowed for “hugging” of the spring, wedging it in place. In the middle of the plate was a hole for the cable to travel through, and at each corner was a 0.5” tapped hole. The first plate was copied four times and used as the top portion of the enclosure.

The second plate (the slider plate) also featured a cupped seat for the spring. The center hole was smaller so the cable could be run through and be crimped on the other side. The four holes at each corner were slightly larger than the tapped holes to act as sliders.

The third plate only featured the tapped holes that were present on the first plate. The third plate was to be used as the mount to the base and to the top plate. It featured two holes used to bolt to the spring traverse mechanism.

The three plates were joined with steel 12” long 0.5” threaded rod. The top and bottom plates were threaded, making them rigid. The middle plate could slide along the rods with the spring between it and the top plate. Then the steel cable was routed through the holes and crimped, ready to be installed on the chair. Later, the enclosures were taken apart to press PVC pipe onto the threaded rods to make the traverse of the middle plate smooth and silent.

The second spring enclosure prototype was tested using an Instron universal testing machine to determine how it would behave within the BoS chair mechanism. Figure 2.15 showcases the spring at three successive intervals of the test. The connection ends of the spring enclosure were attached to the pulling leads of the Instron machine using nylon rope with bowline knots. Bluehill software was used to control the test and record the data. The slack was removed from the ropes leaving a resting force of 25.647 N (about 5 lbs.). The test was begun by expanding the spring at a steady rate. As the spring moved, it was monitored for binding and flexing. The mechanism was seen to be free of any such failure modes.

Figure 2.15: Various images showing how the spring reacted.

When the Instron test reached 130 lbs., one of the bowline knots failed. The spring enclosure was removed from the machine and reattached with more robust knots. The incident provided some insight on what to expect from the forces on the spring connections, and helped drive the decision to use steel cables in the future. The test was then repeated with successful results. The spring withstood a force of 854 N (about 200 lbs.) at 178 mm of displacement. The data from the test was used to compare the spring load to the amount of displacement. This comparison in Figure 2.16 showed an approximately linear progression indicating that the spring enclosure design was operating properly. Following this successful test, the four final spring enclosures were constructed.

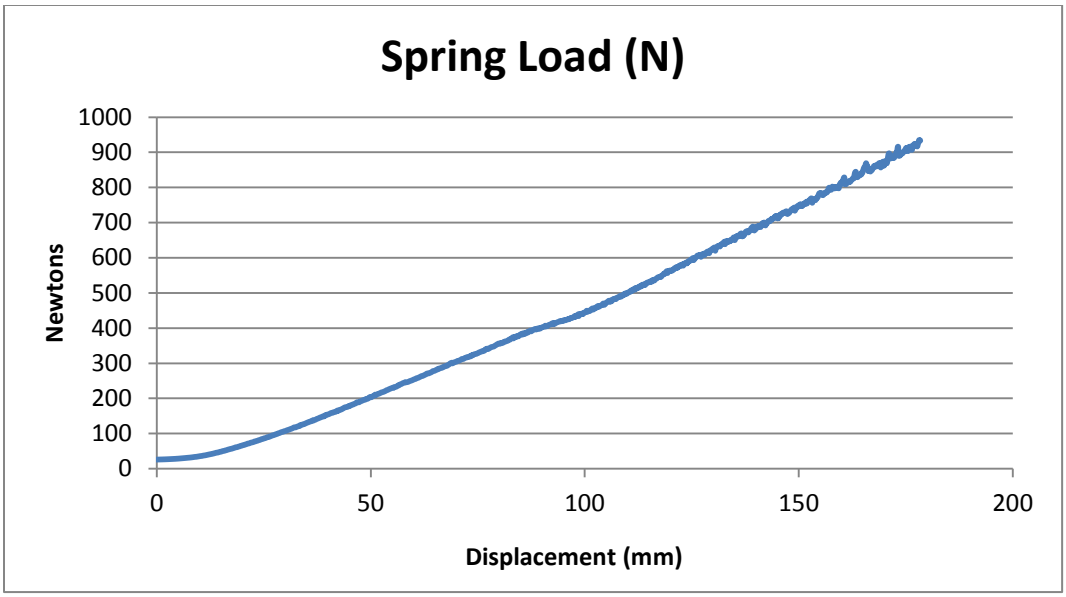

Figure 2.16: Graph of the spring load observed.

2.2.8 Base design and fabrication

The base consists of the stationary components below the pivot point, which includes the base plate and upright column. The base plate is made of a solid piece of steel of the same dimensions as the pivot plate. General purpose low-carbon steel was primarily chosen to increase the weight of all non-moving components below the pivot point. The extra weight was intended to stabilize the chair and prevent any displacement of the chair's location on the ground. The plate itself was unmodified except for 4 threaded holes for mounting the upright column, and several smaller threaded holes for mounting the springs. Figure 2.17 illustrates the base components in relation to the full design.

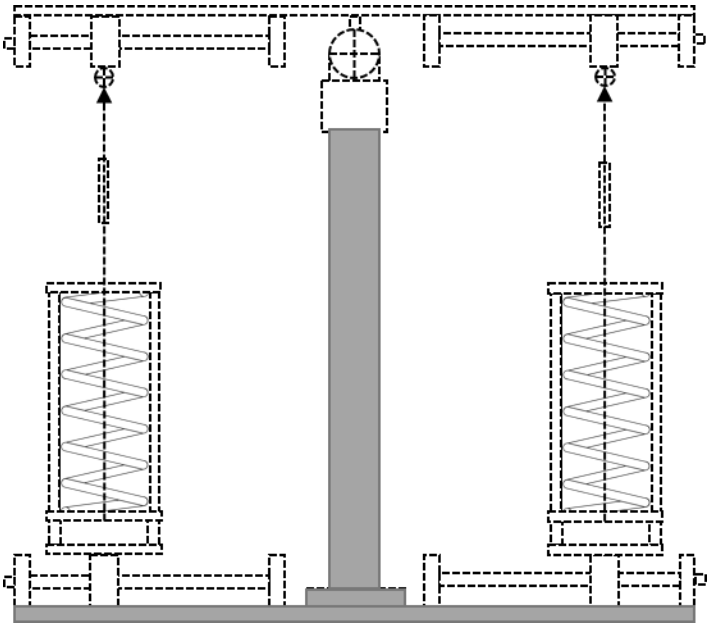

Figure 2.17: Isolated view of base.

A section of Telespar 3” steel square tubing was cut to 2’ in length. A 6” square steel plate was then cut with an opening to insert the beam. Four holes were also cut congruent to the holes in the base plate. The beam was inserted into the 8” plate and welded in place. Then the welded column was firmly bolted to the base plate by matching the four holes to the threaded holes in the base plate.

The final piece needed to connect the base to the pivot plate was made of aluminum so that it could easily be machined. The adapter was inserted into the upright column and bolted to the ball joint on the other side. A 6” square block of aluminum was milled to have a 4” insertion plug on one side and four threaded holes on the other side. The adapter was pressed into the column, and the ball joint bearing the pivot plate was attached. Figure 2.18 depicts the base being tested with only one spring installed.

Figure 2.18: Image of the initial spring load test.

The base weighed approximately 90 lbs. with a footprint spanning 1.0 to 1.4 feet from the central post. The weight and footprint proved to be sufficient to stop any unwanted displacement and sway in the chair. The 90 lb. weight does not include the later added mechanisms or the pivot plate section. Rubber pads were later adhered to the bottom of the base plate to enhance the chair's resistance to displacement. The pads chosen were very dense and thin to ensure that they did not compress under extreme loads, causing extraneous movement.

2.2.9 Spring traverse design and fabrication

The means to move the spring enclosures back and forth to change difficulty was achieved through the use of ACME threaded rod. 6' sections of 0.5" (10 Acme size) threaded rod were cut into eight 10" sections. Both ends of each rod were turned on a

lathe to remove the threads. With the threads removed, the ends could be inserted into 5/16” needle bearings. Simple 2” square blocks of aluminum were milled to mount the bearings.

Eight 1” brass cylinder nuts were pressed into small 2” x 2” blocks of aluminum. The threaded rod was screwed partially into the cylinder nut and then pressed into the bearings. The bearing mounts were bolted into the main base plate of the chair. 0.5” nuts were welded to the outside end of each threaded rod to provide a connection point for the adjustment tool. Figure 2.19 identifies the locations of the traverse mechanisms in relation to the full design.

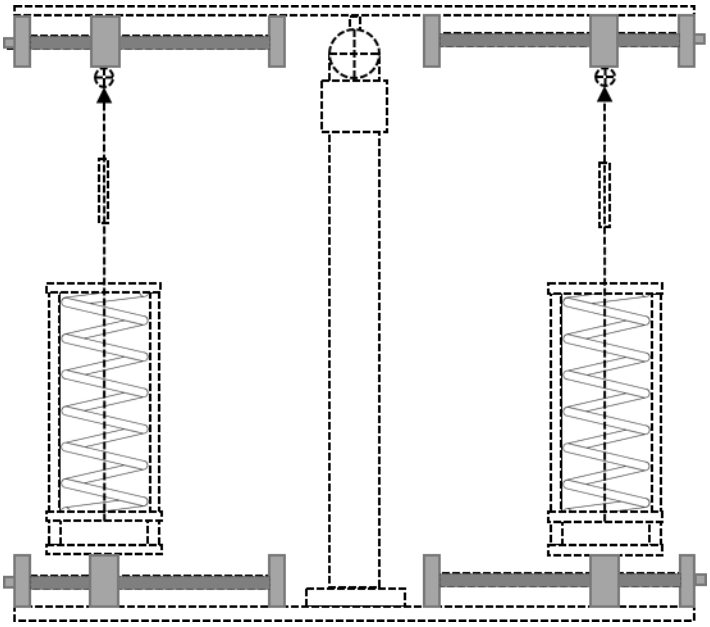

Figure 2.19: Isolated view of the traverse mechanisms.

The completed traverse mechanisms allowed for 6.5” of travel toward or away from the center of the BoS chair. The springs distance could be changed by turning the threaded rods one at a time. The displacement was measured by counting the number of turns incurred. A chart was used to comparatively calibrate the spring displacement and

the measurements are listed in Table 2.1. The chart applies turn increments of two and a half, to achieve a 5% change in difficulty. ***Difficulty*** is interpreted as the percent of displacement out of the possible 6.5”. ***Displacement (in)*** is the change in distance from the outer-most spring position (lowest difficulty). ***Critical distance (in)*** is the actual distance of the spring from the center of the chair at ***Displacement N***.

Table 2.1: Chart used to decipher the number of turns progressed.

Turns	Difficulty	Displacement (in)	Critical
2.5	5%	0.325	9.425
5	10%	0.65	9.1
7.5	15%	0.975	8.775
10	20%	1.3	8.45
12.5	25%	1.625	8.125
15	30%	1.95	7.8
17.5	35%	2.275	7.475
20	40%	2.6	7.15
22.5	45%	2.925	6.825
25	50%	3.25	6.5
27.5	55%	3.575	6.175
30	60%	3.9	5.85
32.5	65%	4.225	5.525
35	70%	4.55	5.2
37.5	75%	4.875	4.875
40	80%	5.2	4.55
42.5	85%	5.525	4.225
45	90%	5.85	3.9
47.5	95%	6.175	3.575
50	100%	6.5	3.25

2.2.10 Control cable design and fabrication

Four steel cables were cut to the general length from the bottom of the spring to the corresponding contact on the pivot plate. The cable was 1/16” in diameter, rated at approximately 200 lbs. A turnbuckle was installed mid-length of the cable to make cable length adjustments fast and simple. When the cables were attached in the final build, they

were adjusted so the springs were minimally engaged to remove excess play in the pivot plate.

2.2.11 Safety frame control design and fabrication

The safety frame was designed to be a lightweight and sturdy enclosure able to protect the participant when he or she falls during the experiment. The construction consists of a sturdy lightweight wooden frame with plywood impact boards that are covered with thick foam. The impact boards are slanted to catch participants at the final allowable angle of their fall and to safely hold them in position until they return to the upright starting position. The incline would also prevent the participants from falling off of the chair, avoiding potential injury and a lengthy process involving climbing back on the chair.

The safety frame was designed as four interlocking pieces, so that it can be easily disassembled and moved. The lowest part of the impact board was designed to overlap the bottom edge of the chair. The board was offset at a distance to allow for the pads to exist without contacting the chair. This feature closed the gap at the bottom so participants could not fall below the chair and frame. The top of the impact board was measured to a distance approximately one foot greater than the projected impact position of a 6’ participant’s head. The planes were inclined at 45°.

The structures of the four frames were constructed from 2x4 lumber, fastened with wood screws. All fastening locations were predrilled to ensure that the wood screws did not split the wood, thus avoiding potential safety concerns. Each impact board was made of one sheet of 0.5” thick plywood. The board was cut into a trapezoidal shape to fit the design. To ensure that the angled boards fit together properly, miter angles were

calculated for the cuts. The desired result was to make the edges meet like an inverted square pyramid. The result of the miter angles is highlighted in red in Figure 2.20, depicting the completed frames without padding.

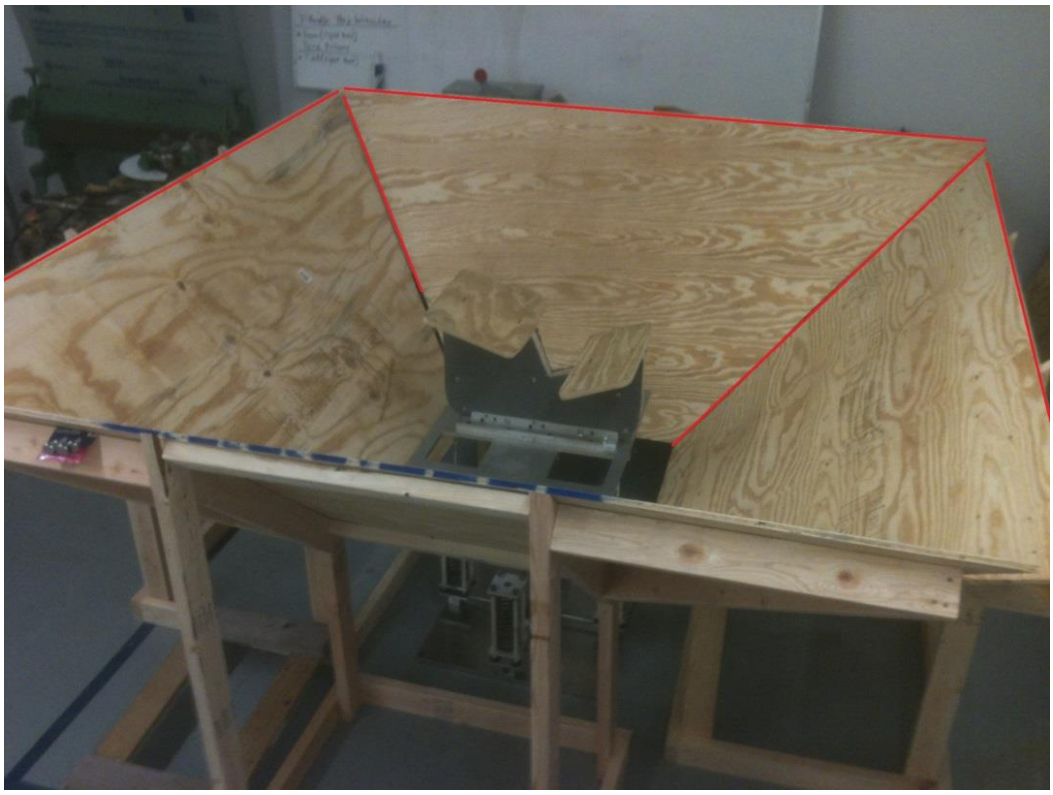

Figure 2.20: Image of the wood frames arranged around the chair.

8” thick couch cushion foam was purchased to cover the plywood. The cushion needed to be very thick to ensure that the participant would remain comfortable and not impact the plywood beneath. Cushion of this thickness could not be obtained in the size necessary to fully cover the plywood surfaces of the safety frame. Therefore, smaller sections of foam were cut and fitted together to cover the plywood. To ensure that there were no gaps in the corners where the angled surfaces meet, miter angles were calculated. The desired dimensions were then traced onto the foam with a marker.

To cut the foam, a wire burning kit was assembled from basic materials. The kit consisted of a power supply, and a cutting device. The cutting device was constructed of 2x4's formed in the shape of a "U" with a steel wire running the length of the open end. The steel wire was used as the foam cutting element. The steel wire was connected to the power supply to generate a current that heated the wire. Different lengths and thicknesses of the cutting wire were tested and the final wire was found to demand approximately 12V at 1.5A from the power supply. The power supply was turned on, set to 12V 1.5A and turned off. Then the cutting element was connected and the power supply was turned back on. The current was then adjusted until the wire just began to glow red. At that point, the wire was hot enough to cut foam, but not hot enough to burn or ignite it. The foam was cut by guiding the cutting element along the traced lines on the surface of the foam. Three pieces of cut foam were placed on each of the four impact boards as shown in Figure 2.21. Two large trapezoidal pieces were laid down side-by-side with one triangular piece to finish the missing corner.

Figure 2.21: Image of the foam installed after cutting.

To finish the safety frame, the foam needed to be covered. Queen size flat sheets were used to protect the foam and to hold it in place. The covers would also make the padding easy to clean, and appear aesthetically pleasing. Each sheet was laid onto a large workbench and the foam was laid upside-down on top of it. Then the sheet was wrapped and fastened around the foam pieces to hold them together as if being upholstered. The top edge of the sheet was left unfastened. The bundled foam and sheet were then placed back on the frame and shifted into place. The unfastened top piece of the sheet was clipped to the top of the frame to hold the padding in place. When the four frames were pushed together, the interlocking pyramidal shape held the pads in place as well. The four completed frames are shown in Figure 2.22 with their covers installed.

Figure 2.22: Image of finished safety frame after being upholstered.

2.2.12 Adjustment tool design and fabrication

The final piece needed to make the chair function was a tool that could turn the adjustment screws to change the difficulty. The 0.5” nuts welded to the end of the adjustment screws made it feasible to use a wide range of tools for the adjustment.

Wrenches, ratchets and power tools were considered. However, a tool was needed that could be quickly inserted to make a swift adjustment, given the constraints of the chair. The configuration consisted of: one speed handle, two extension bars, one universal joint, and one 0.5” 12-point socket. The components are shown together as the completed device in Figure 2.23.

Figure 2.23: Image of the assembled adjustment tool.

This configuration was chosen for multiple reasons. The speed handle made swift adjustments possible. This tool provided the ability to easily count turns. Turns could be counted when rotating 360° from top-dead-center, otherwise known as the 12 o’clock position. If smaller adjustment increments were needed, half turns could be counted every 180° alternating between 12 o’clock and 6 o’clock. The safety frame made it very difficult to access the adjustment screws. Thus, it was necessary to add extension bars to the tool. The extension bars made it possible to make adjustments while standing outside of the frame at all times, improving the speed of adjustments. Figure 2.24 depicts the adjustment tool being applied to the lower adjustment screw at an angle, making adjustments easier. Figure 2.25 portrays the necessity of the tool, as the upper adjustment screws were very difficult to reach.

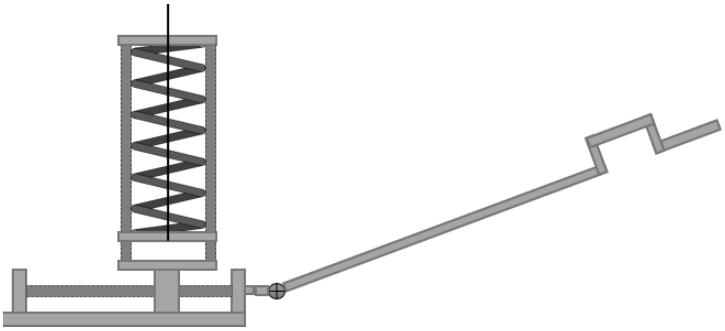

Figure 2.24: Diagram of the tool being applied to a lower traverse mechanism.

Figure 2.25: Image of the tool being applied at an angle to the upper traverse mechanism.

The completion of the safety frame marked the final task needed to finish construction of the BoS platform. With these preparations completed, it was then time to begin preliminary testing. The BoS testing platform is shown from a distance in Figure 2.26, consisting of the BoS chair and safety frame.

Figure 2.26: Image of the completed BoS testing platform.

CHAPTER 3: METHODS

Two testing methods were used to evaluate the operation of the BoS chair, the Threshold of Stability test and the Basin of Stability test. These two tests were performed back-to-back in the same test protocol. Results from the ToS test were used to determine how the BoS test would be run.

3.1 Spring difficulty logic

Several related dimensions were used in this study. The critical dimensions used are displayed in Figure 3.1. $\boldsymbol{d_{comp}}$ is defined as the distance of the spring from the 0% difficulty position. The value is complementary to the critical distance. The sum of the critical and complementary distances is always 10.5". The critical distance ($\boldsymbol{d_{crit}}$) is the distance from the central pivot point of the chair to the spring when ToS is achieved. The critical distance is a measure of the participant's balance control ability to overcome instability. Distance equilibrium ($\boldsymbol{d_{eq}}$) is the spring distance where static equilibrium at any angle can be achieved without human balance control. Thus, the equilibrium distance is a quantitative measure of the height and weight of the subject. This equilibrium distance may lie beyond the scale (testable range) of the BoS chair, and can only be calculated. The normalized critical distance ($\boldsymbol{d_{norm}}$) is the percentage of the equilibrium distance where $\boldsymbol{d_{crit}}$ lies.

$$\boldsymbol{d_{norm} = \frac{d_{crit}}{d_{eq}} = d_{eq}} \quad \textbf{(1)}$$

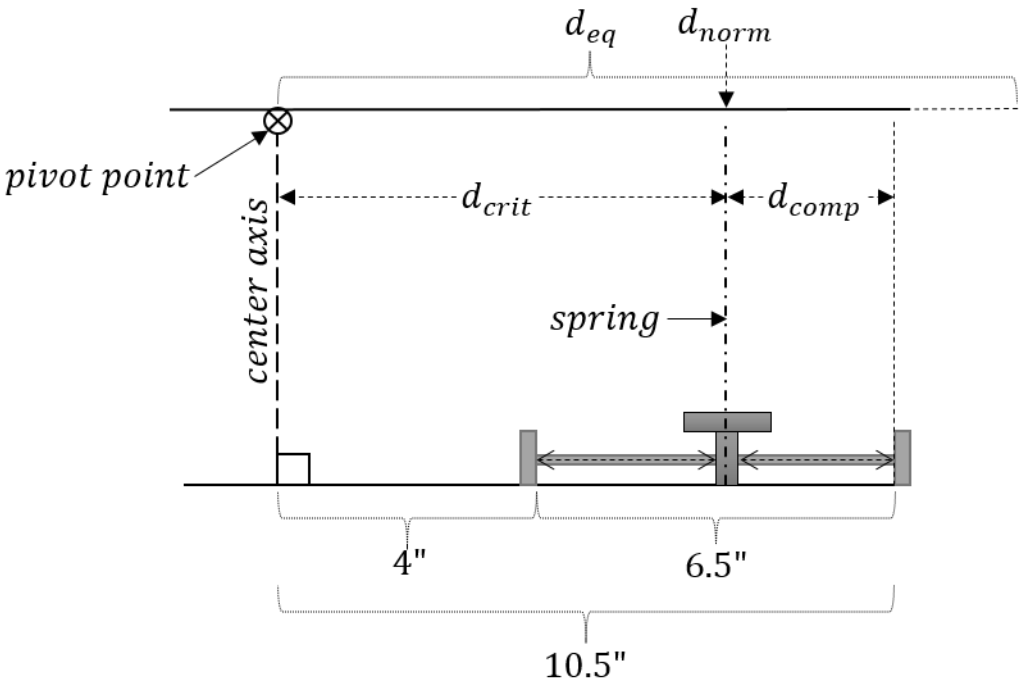

Figure 3.1: Diagram of spring locations in relation to the central pivot point.

3.2 Equilibrium normalization

In theory, different size participants with equal balance capability will have different values of $\boldsymbol{d_{crit}}$ because of their difference in size. Stated another way, if two people were to be tested at the exact same spring setting, the person of greater mass would experience more difficulty, regardless of their ability to balance, and would appear to have less balance capability.

As mass increases, so does difficulty. Thus, height and weight may be a confounding factor in the results that may mask differences in balance control capability. This correlation will be analyzed to determine if it is significant. If it is significant, then normalization must be performed to nullify or reduce this effect. Without normalization, it would be hard to differentiate the real performance between each participant, because it

is unknown how mass and height influenced the result. Normalization is intended to account for mass and height differences for all participants so their actual performance capability can be compared directly.

An analysis of the chair design in static equilibrium was performed. The system model was set at an arbitrary deflection angle, $\boldsymbol{\theta}$, and spring and body forces were applied in Figure 3.2. The spring force, $\boldsymbol{F}$, is produced by compressing the springs as $\boldsymbol{\theta}$ increases. This provides a stabilizing moment around the pivot point. In contrast, body weight, $\boldsymbol{W}$, and the weight of the upper chair assembly produce a destabilizing moment around the pivot point.

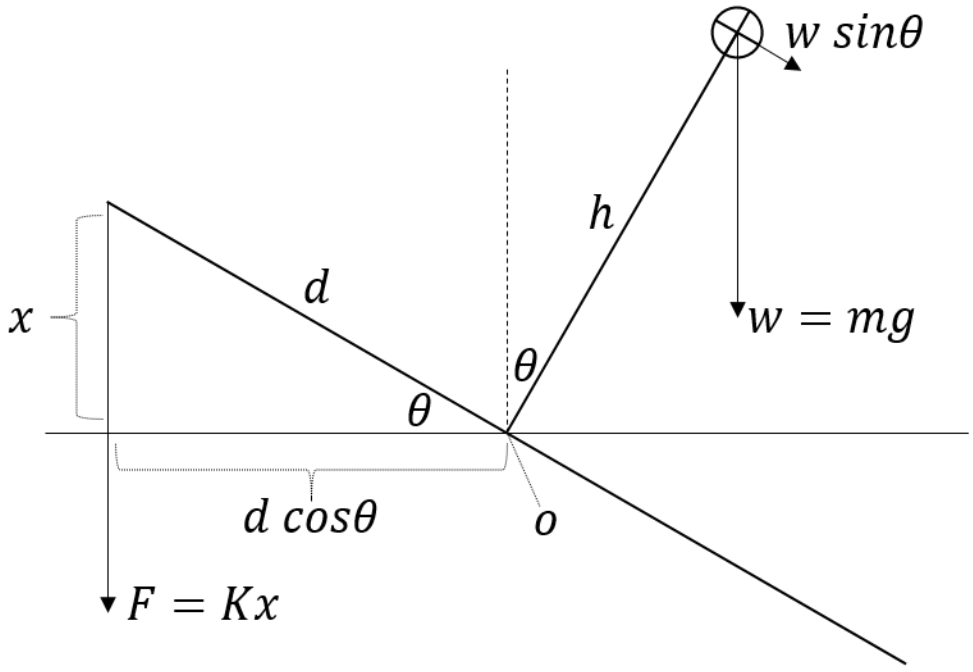

Figure 3.2: Diagram representing deflection of the chair with the participant center of mass resting at the top

For static equilibrium, the sum of the moments about the pivot point (***o***) must be equal to zero,

$$\Sigma M_o = 0. \quad (1)$$

and

$$F \cdot d\cos\theta - hw \cdot \sin\theta = 0. \quad (2)$$

Substituting ***kx*** for the force and ***mg*** for the weight, and where ***d*** is the distance in inches,

$$Kx \cdot d\cos\theta - h(mg)\sin\theta = 0. \quad (3)$$

However, from trigonometry the spring compression can also be expressed in terms of ***d***,

$$\sin\theta = \frac{opposite}{hypotenuse} = \frac{x}{d}, \quad (4)$$

so,

$$x = d\sin\theta. \quad (5)$$

Substituting the ***x*** yields,

$$K(d\sin\theta) \cdot d\cos\theta - mgh\sin\theta = 0. \quad (6)$$

Dividing by the $\sin\theta$ and combining terms,

$$Kd^2\cos\theta - mgh = 0. \quad (7)$$

For the purposes of the research, primary interest was in stability around the vertical equilibrium position where theta was small. In Figure 3.3, for a small θ, $\cos\theta \approx 1$.

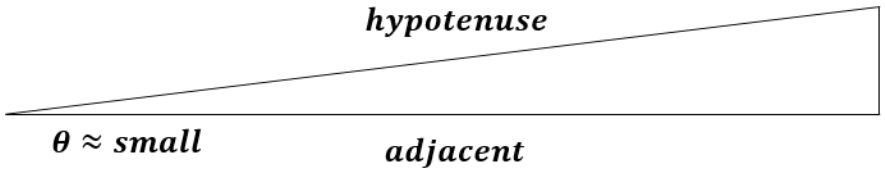

Figure 3.3: Representation of a small angle being approximated to zero.

When θ is small, the hypotenuse is approximately equal to the adjacent line and their quotient is ***1***.

$$\boldsymbol{cos\theta = \frac{adj}{hyp} \rightarrow cos\theta \approx 1.} \quad \textbf{(8)}$$

So,

$$\boldsymbol{Kd^2(1) - mgh = 0,} \quad \textbf{(9)}$$

simplify,

$$\boldsymbol{Kd^2 - mgh = 0.} \quad \textbf{(10)}$$

Equation (10) may be solved for $\boldsymbol{d}$.

$$\boldsymbol{Kd^2 = mgh} \quad \textbf{(11)}$$

$$\boldsymbol{d^2 = \frac{mgh}{K}} \quad \textbf{(12)}$$

$$\boldsymbol{d = \sqrt{\frac{mgh}{K}}}\,. \quad \textbf{(13)}$$

The equilibrium displacement ($\boldsymbol{d_{eq}}$) is defined as,

$$\boldsymbol{d_{eq} = \sqrt{\frac{m_s g h_{com}}{K}}}\,. \quad \textbf{(14)}$$

For a given participant subject, s. The distance from the pivot point to the center of mass of the subject while kneeling on the BoS chair is $\boldsymbol{h_{com}}$. Its value is approximated by one third of the subject height $\boldsymbol{h_s}$.

$$\boldsymbol{d_{eq} = \sqrt{\frac{m_s g h_s}{3K}}}\,. \quad \textbf{(15)}$$

Because the weight of the subject was measured, it can be substituted back into the equation.

$$\boldsymbol{w = mg \rightarrow m = \frac{w}{g}.} \quad \textbf{(16)}$$

This yields the equation for $\boldsymbol{d_{eq}}$ which is used as a normalizing factor to account for differences in body weight and height.

$$\boldsymbol{d_{eq} = \sqrt{\frac{w_s h_s}{3K}}} \quad . \tag{17}$$

The threshold (ToS) percentage for each participant was a derivative of the complementary spring distance. To convert the percentage back to inches, it was multiplied by total spring travel (6.5”).The threshold (ToS) percentage for each participant was a derivative of the complementary spring distance. To convert the percentage back to inches, it was multiplied by total spring travel (6.5”).

$$\boldsymbol{d_{comp} = ToS(Cp) \cdot 6.5.} \tag{18}$$

The critical distance was then obtained by subtracting the constant sum of the critical and complementary distances (10.5”) by the previously obtained complementary distance.

$$\boldsymbol{d_{crit} = 10.5 - d_{comp}.} \tag{19}$$

The equilibrium distance was calculated by referencing subject height and weight, while factoring in a spring constant of 42 pounds per inch, and a divisor of 3. 3 is the approximate mass at kneeling height in inches.

$$\boldsymbol{d_{eq} = \sqrt{\left(\frac{hw}{3 \cdot 42\frac{lbf}{in}}\right)}.} \tag{20}$$

The normalized distance is simply the critical distance divided by the equilibrium distance, and displayed as a percentage.

$$\boldsymbol{d_{norm} = \frac{d_{crit}}{d_{eq}}.} \tag{21}$$

Minitab (Rev. 16, Minitab Inc., State College, PA) was then used for statistical analysis.

3.3 Test protocol

Preliminary tests were necessary to gauge the difficulty levels and address any issues that may be found in the mechanism. Xsens motion tracking software was tested and configured on a laptop computer using the Xsens MTi motion tracker. The software collected three dimensional angular data (roll, pitch, and yaw) over time. The testing protocol consists of two separate tests. The Threshold of Stability test and the Preliminary Basin of Stability test were to be performed consecutively for every participant. The results from the ToS were used to determine the set points for BoS test.

3.3.1 Study participants

Twelve young adults from the university and surrounding areas were recruited for testing. All participants were healthy individuals between the ages of 23 and 26 and their general information is listed in Table 3.1. Participants were asked to wear long pants and closed-toe shoes before entering the testing area. The participants were then asked if they would like to provide their known height, weight and age for the datasheet. Lastly, participants were asked to review the IRB consent form, as it was explained by the researcher. Participants were told about the process, the risks involved, and what to do if they had any concerns.

Prior to beginning the test, all participants signed an informed consent form approved by the Institutional Review Board at Western Carolina University. Participants ranged from very small framed females to larger framed males.

Table 3.1: Participant demographics.

Subject	Gender	Age (yrs)	Weight (lbs)	Height (in)
1	M	24	154	68
2	M	24	143	73
3	F	23	128	63
4	M	22	190	72
5	F	22	144	61.2
6	F	30	110	64.8
7	M	24	170	74
8	F	20	170	64.8
9	F	28	138	66.5
10	F	20	130	63.6
11	M	24	182	70
12	M	24	230	75
Avg.		23.8	157.4	68
SD		2.9	32.9	4.7

3.3.2 Threshold of Stability test protocol

One preliminary test was attempted with a student who would not be featured in the final results to calibrate the testing device and look for flaws. The proposed protocol was simulated in the test, and then optimized as needed. A total of two hours were spent experimenting with the adjustments and practicing falls and ensuring that the device was comfortable for the participant. In the following days, the protocol was completed and the chair was prepared for final testing with only minor adjustments.

Final testing began the week following the preliminary tests. Given the results of the preliminary test, the target time for each participant's trials was 45 minutes. Testing days were selected at the participants' leisure, based on their schedule. Most tests were performed in late afternoon hours to ensure that nearby lab spaces would not be in use, minimizing possible distractions. Most tests were performed two per day, consecutively, to retain personnel in fewer engagements.

The student who assisted with the preliminary test served as an assistant in the first two participants' trials. The assistant's duty was to help the participant climb onto the chair, and to answer any questions the participant might have. The assistant was also needed for various other tasks, such as data recording (most of my time was spent making adjustments and watching the trials). The first two participants were then recruited as assistants to relieve the first assistant, as they had gained the knowledge necessary to assist in the trials. One male assistant and one female assistant were chosen.

Participants were instructed with the recommended method of mounting the chair, which was occasionally demonstrated. When the participant was seated, they were asked to hold the support rope from above to remain stable while the safety frame was secured. Once secured, the participant was asked to cross their arms at chest-height with hands resting on the shoulders. The rope was pulled away from the testing area. They were asked to concentrate by looking straight forward at an object or point on the wall and begin trying to balance. Prior to data collection, participants were allowed to fall a few times to become comfortable with the device. Extra cushions were offered for more comfort if needed, however, most participants did not request it.

With the setup complete, the first trial of the ToS experiment started immediately to avoid participant fatigue. The chair was set to the first difficulty setting, as directed by the data sheet, before the arrival of any participants. The participant was asked to balance. If the participant fell, the rope was lowered, and the time was stopped. A fall before 60 seconds elapsed indicated a failure, and an "F" was recorded on that specific setting for that trial. If 60 seconds had passed without the participant falling, the data was

marked as a “P” for pass. Then the rope was lowered so the participant could stabilize and rest, while adjustments were made.

The sequence for recording and proceeding with results of each trial is outlined in Figure 3.4. The figure represents a flow chart guiding the procedure. The flow chart starts at “TEST” and ends at “END.”

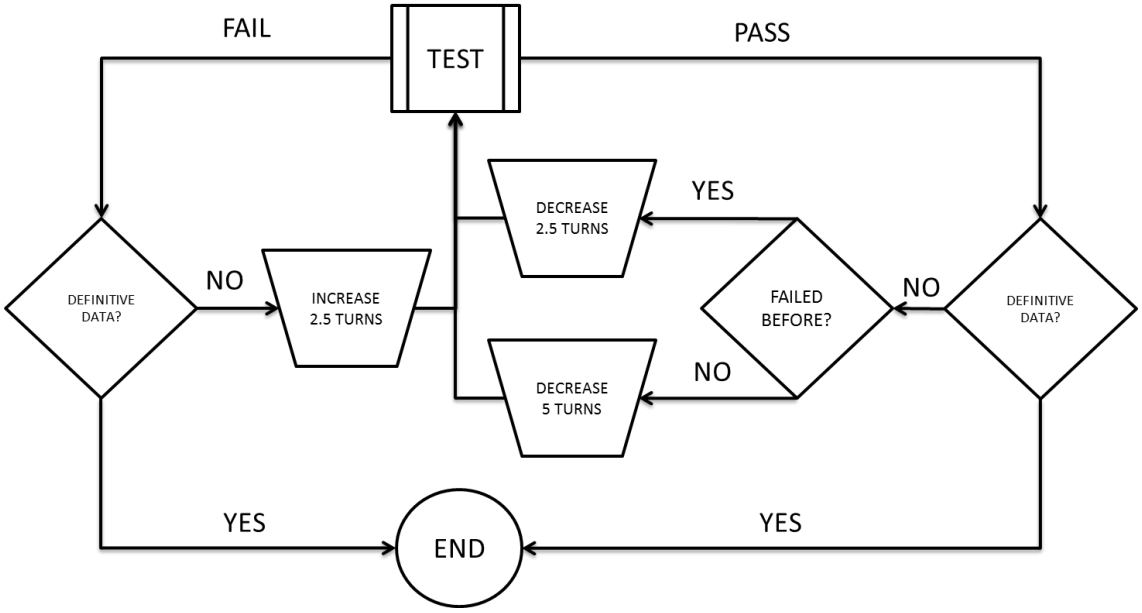

Figure 3.4: Flow chart indicating the ToS process.

The flow chart determines the sequence of difficulty levels to be tested. All tests started at 40% difficulty. When each 60 second trial was completed, it was determined as either failing or passing. The scenarios represented by the flow chart are explained as follows:

PASS

The participant has successfully balanced for 60 seconds.

FAIL

The participant has failed to maintain balance for 60 seconds.

$$\boldsymbol{PASS\ or\ FAIL\ \rightarrow\ DEFINITIVE\ DATA?}$$

Definitive data represents the moment to decide if there is sufficient data to end the trials. This requires a threshold to be found on the data sheet.

$$\boldsymbol{PASS\ or\ FAIL \rightarrow DEFINITIVE\ DATA? \rightarrow YES \rightarrow END}$$

Sufficient data is collected when the participant has achieved two passes at one difficulty, and two failures as a consecutive greater difficulty. Assuming definitive data has not yet been collected, NO is followed along the flowchart to the next steps.

$$\boldsymbol{PASS \rightarrow DEFINITIVE\ DATA? \rightarrow NO \rightarrow FAILED\ BEFORE?}$$

This dialogue box asks if a failure has occurred yet to determine the size of the following increments.

$$\boldsymbol{FAILED\ BEFORE? \rightarrow NO \rightarrow DECREASE\ 5\ TURNS \rightarrow TEST}$$

This pattern is expected to occur over the first few trials until the difficulty approaches the participant's threshold. It acts as a fast-forward feature by doubling the increments to get to the threshold more quickly. This is disabled after the first detected failure to begin to focus on a finer difficulty increment of as they get closer to the threshold.

$$\boldsymbol{FAIL \rightarrow DEFINITIVE\ DATA? \rightarrow NO \rightarrow INCREASE\ 2.5\ TURNS \rightarrow TEST}$$

When a failure occurs, the adjustment screw is rewound 2.5 turns to lower the difficulty. The difficulty is lowered until a pass occurs.

$$\boldsymbol{FAILED\ BEFORE? \rightarrow YES \rightarrow DECREASE\ 2.5\ TURNS \rightarrow TEST}$$

After a failure occurs, increases in difficulty progress by 2.5 turns. This also means that when a pass is detected, the difficulty is then increased.

When the ToS was successfully determined, the participant was notified that the test was complete. The participant was then promptly assisted down from the chair for a

rest period. During the rest period, the participant was allowed to walk around and talk to the assistants to relax and relieve tension. During this time, the chair was adjusted for the next test while the laptop was set up for data recording.

The reason tests in the protocol were to start at 40% difficulty and progress at an accelerated rate until a failure occurred was due to the springs used. The springs provided too much resistance, so lower difficulties were simply too easy. These factors were calculated beforehand, but there were too many unknown factors in the design, such as the final weight of the chair. Though the springs were found to be slightly too resistant, the final result was still surprisingly within tolerance, allowing for the trials to be completed. In future tests and uses of the device, the springs can easily be changed for lighter springs. The springs can be changed without any major modification to the geometries and functions of the original mechanism.

Threshold of Stability Testing Sheet

Name:_____
Age: 24
Weight: 190 *lbs. / 220 lbs. max*
Height: 160 *inches*
Sex: Male
Randomization: EH
Participant #: 00

Threshold Detection

- The table has been offset to omit lower difficulties found to be too easy.
- Test in trials of **60 second** durations
  - If successful, record a pass and advance **4 steps (10 turns)**
  - If not successful, record a fail and record time in seconds
  - After the first failure is detected, advance **1 step (2.5 turns)** per trial
- Successively record one value per column
  - When a failure is detected, decrease difficulty
  - When a pass is detected, increase difficulty
  - The highest level Pass is recorded as the Threshold (T)
- Allow **2 minutes** for difficulty adjustment and rest period.
- After completion, average any stacked **P**'s and **F**'s on a repeated difficulty.
- Select the two failure modes for the BoS trials.
  - Easy (E) – record **1** step past ToS (T)
  - Hard (H) – record **3** steps past ToS (T)

P = Pass **F** = Fail

Turn **counter-clockwise** to increase difficulty, Turn **clockwise** to decrease difficulty

Step	Turns	%	T1	T2	T3	T4	T5	T6	T7	T8	T9	T10	T11	T12	Time		BoS	Notes
1	**10.0**	20	P															
2	12.5	25																
3	15.0	30		P														
4	17.5	35																
5	**20.0**	40			P													
6	22.5	45																
7	25.0	50				P												
8	27.5	55																
9	**30.0**	60					P											
10	32.5	65																
11	35.0	70						P										
12	37.5	75																
13	**40.0**	80							P			P					T	
14	42.5	85									F		F				E	
15	45.0	90								F								
16	47.5	95															H	
17	**50.0**	100																

Figure 3.5: Example of the ToS data sheet used for all 12 participants.

3.3.3 Basin of Stability test protocol

The basin of stability test was conducted after the ToS test in the same test session. The participants were given a randomization of two versions of the tests. The first version was to test a harder difficulty before the easier difficulty in the Threshold Analysis Test. The second version was to test the easy mode first. The randomization was split evenly, so there would be no bias, or more of one version than the other. In all, there were four types of data sheets and three copies of each (Male A, Male B, Female A, Female B). All copies were printed before testing began, and then shuffled for randomization.

Trial data was recorded on the data sheet and three points were identified under the "BoS" column. The points were noted as threshold (T), easy (E), and hard (H). Threshold was identified as the last difficulty in which the participant could consistently pass, hence the threshold of stability. A setting of "E" was defined as the first difficulty exceeding the ToS. Hard was identified as a difficulty 10% higher than the easy setting. In some cases only 5% higher was used due to limitations in the device.

The BoS test began shortly after the rest period. During that rest period, the chair was set to one of the easy or hard modes as described above and the laptop was set up for recording. The laptop was to be used to record live feedback from the Xsens device mounted to the chair. The software automatically detected and calibrated the device at launch, displaying what is shown in Figure 3.6.

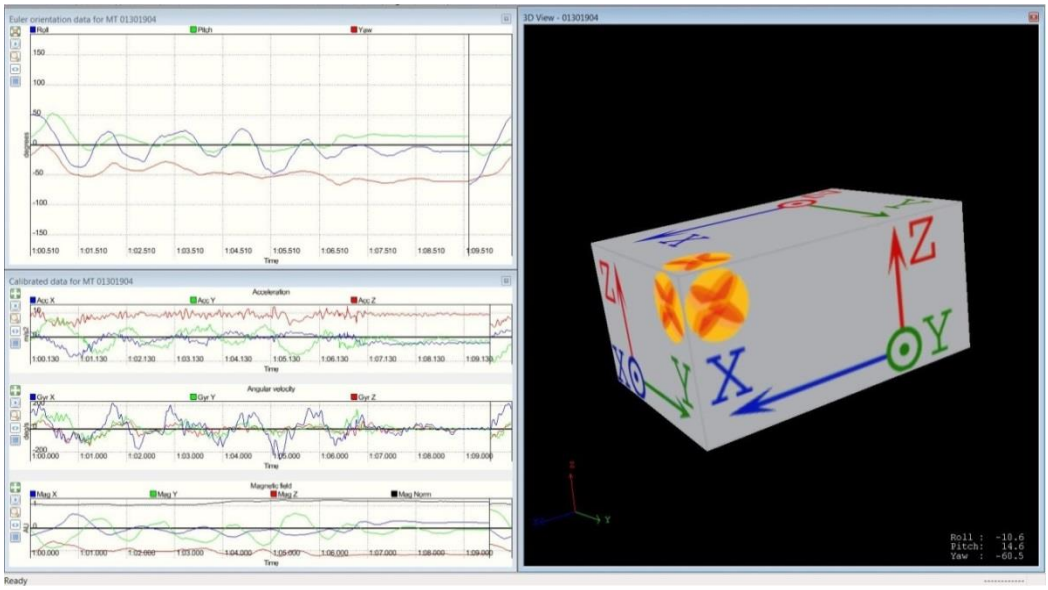

Figure 3.6: Example of X-sens software showing data readouts (left) and a 3D representation of the sensor heading (right).

In the lower right side of the screen, an Euler angle box was visible. The box rendered live feedback from the chair at all times. To test the functionality of the sensor, the chair was tilted sequentially in different directions. As the chair was tilted in each direction, the assistant confirmed that the Euler angle box followed the same motion, and that the surrounding windows showed the coinciding motion in linear form. The last test was then ready to be performed.

The participant was then asked to climb back onto the chair using the same methods as before. The safety frame was closed and the participant was given a new set of instructions. Instead of starting a new trial every time a failure was detected, the trial would continue for two minutes regardless of falls. The participant was asked to use the rope to correct their posture as it was lowered to within their reach with each fall. After a fall, the participant had to regain stability and assume the recognized balancing position, with arms crossed and hands on shoulders. Fall times and posture correction times were

to be recorded throughout the trials. The protocol called for detection of at least four falls in the course of two minutes. One minute rest periods were required between trials to avoid fatigue. If four falls were not detected, then the trials would be repeated until four cumulative falls were detected across all trials of the same difficulty. When the four falls were attained, the chair was then set to the other difficulty level. The trial was then repeated.

If a participant's trial failed to yield what was considered sufficient data (at least four falls per difficulty), more data sets were recorded until the requirements were met. This resulted in as many as three data sets for some participants. For instance, the harder difficulty for one participant might have yielded four falls in the first two-minute trial. However the easier difficulty might have required as many as three two-minute trials to achieve four falls. The reason for this was that the lower level of difficulty might have been too easy to have the participant fall frequently enough.

During the BoS test, as the participant began to balance, the lab assistant awaited instruction to start recording. The instant that the participant appeared to be stable, the lab assistant was silently signaled to record. The trial ran for the allotted two minutes, as everyone remained quiet. The reason that data collection was not started until the participant was stable was to obtain consistent data. If the start and stop portions of the trial were included in the recorded data, false movements would be recorded in the transition from stable to unstable. In other words, it took a moment for the participant to attain the natural state of balance that we wanted to analyze. The Basin of Stability chair was successful in gathering data. The files yielded were raw text documents consisting of point cloud data.

Basin of Stability Testing Sheet

- Create a folder for each participant by participant number.

  Folder Name:_____(Participant ##)

- Run **2 Minute** trials.

1. Record easy failure mode:

   Easy: 85
   Save As: **P## Easy**

   Falls:

   1 -_____

   2 -_____

   3 -_____

   4 -_____

2. Record hard failure mode:

   Hard: 95
   Save As: **P## Hard**

   Falls:

   1 -_____

   2 -_____

   3 -_____

   4 -_____

Figure 3.7: Basin of Stability sheet used to count and record fall times.

CHAPTER 4: RESULTS & ANALYSIS

4.1 Overview of results

The new BoS Chair was used to determine the Threshold of Stability test for normal healthy young adults. The purpose of this test was to establish a baseline for normal people. In future studies, performance of people with disabilities, low back pain, or musculoskeletal abnormalities will be compared to the baseline to determine how they differ from the normal population. Performance before and after treatment can be compared to determine if the treatment improved their performance, i.e. their performance was closer to normal. In addition, several post-hoc analyses were performed. An evaluation was conducted to determine if differences existed based on gender and the effect of weight and height were studied to determine their effect on the calculated parameters. The basin of stability test was used to collect preliminary data that will be used to determine the size of the torso BoS.

4.2 ToS testing results

Data from the twelve subject data sheets were put into a spreadsheet. The data sheets provided subject gender, age, weight, height, and the measured ToS capability. With core data imported to the spreadsheet, the additional parameters were calculated (complimentary distance, critical distance, equilibrium distance, and normalized distance). Once the data derived from the ToS experiment was compiled, it was statistically analyzed for the validity of normalization.

The threshold of stability for normal healthy young adults was found to have a mean value of d_{crit} = 4.5" with a standard deviation of 0.66" (Table 4.1). The d_{crit} value for males was higher, d_{crit} = 4.77" with a standard deviation of 0.57. The value for females was found to be lower, d_{crit} = 4.23" with a standard deviation of 0.68. The smallest participant was 65" at 110 lbs. The largest participant was 75" at 230 lbs. It was observed that participant size seemed to have an effect on their ability to balance, ToS capability and d_{crit}. These results signified a need to analyze differences in gender, and participant size.

Table 4.1: Compiled ToS results.

Subject	Gender	Age (yrs)	Weight (lbs)	Height (in)	ToS (Cp)	d_comp (in)	d_crit (in)	d_eq (in)	d_norm
1	M	24	154	68.0	80%	5.20	5.30	9.12	58.1%
2	M	24	143	73.0	80%	5.20	5.30	9.10	58.2%
3	F	23	128	63.0	95%	6.18	4.33	8.00	54.1%
4	M	22	190	72.0	75%	4.88	5.63	10.42	54.0%
5	F	22	144	61.2	85%	5.53	4.98	8.36	59.5%
6	F	30	110	64.8	95%	6.18	4.33	7.52	57.5%
7	M	24	170	74.0	85%	5.53	4.98	9.99	49.8%
8	F	20	170	64.8	70%	4.55	5.95	9.35	63.6%
9	F	28	138	66.5	90%	5.85	4.65	8.53	54.5%
10	F	20	130	63.6	75%	4.88	5.63	8.10	69.4%
11	M	24	182	70.0	80%	5.20	5.30	10.06	52.7%
12	M	24	230	75.0	60%	3.90	6.60	11.70	56.4%
Avg.		**24**	**157**	**68.0**	**81%**	**5.25**	**5.25**	**9.19**	**57%**
SD		**3**	**33**	**4.7**	**10%**	**0.66**	**0.66**	**1.20**	**5%**

4.3 ToS datasheet results

ToS data sheets proved to be very useful in keeping track of the trial sequence for each participant. The data sheets were essential in determining the ToS value for each of the twelve participants. An example of one male participant in Table 4.2 shows a

progression that was typical in most trials. Starting at 40% difficulty, the difficulty was increased 20% each time the participant passed. The male subject failed on the third trial at 80%, resulting in a 5% decrease in difficulty for the next trial. With the first failure detected, it can be assumed that the ToS is close. Therefore all difficulty changes continued at the smaller increment (5%). The male subject progressed this way until two failures and two passes were detected within 5%. The two passes were at an 80% difficulty and the two failures were at an 85% difficulty. These results show the ToS to be 80% difficulty. The results showed very little irregular deviation.

Table 2.2: Example of a male ToS results, Easy-Hard (Participant 11).

Step	Turns	%	T1	T2	T3	T4	T5	T6	T7	T8	Time		BoS	Notes
1	**10.0**	20												
…	…	…												
5	**20.0**	40	P_1											
6	22.5	45												
7	25.0	50												
8	27.5	55												
9	**30.0**	60		P_1										
10	32.5	65												
11	35.0	70												
12	37.5	75				P_1								
13	**40.0**	80			F_1		P_1		P_2		30		**ToS**	2 passes √
14	42.5	85						F_1		F_2	5	7	E	2 fails √
15	45.0	90												
16	47.5	95											H	
17	**50.0**	100												

Irregular deviation is defined when a repeated difficulty yields a different result, causing excessive back and forth progression through difficulties. It is caused when a participant cannot consistently achieve the same performance at repeated difficulties. As seen with the previous male subject, 80% difficulty was first detected as a failure, but the

following two trials at the same difficulty were detected as passes, yielding the ToS. This was regarded as minor irregular deviation, as it was just one occurrence throughout the testing session. Only one participant experienced excessive deviation in Table 4.3. This particular female subject reversed in difficulty from 95% three times consecutively, and then progressed back to 95%. This caused a pyramid shape to appear on the data sheet. This repetition of difficulties was regarded as more irregular than others, but ToS was still recorded successfully without breaking protocol. It could possibly be inferred that the subject had a balance control deficiency, but unlikely since the participant may have just been uncomfortable or unfamiliar with the BoS chair.

Table 4.3: Example of a female ToS result, Hard-Easy (Participant 09).

Step	Turns	%	T1	T2	T3	T4	T5	T6	T7	T8	T9	Time		BoS	Notes
1	**10.0**	20													
…	…	…													
5	**20.0**	40	P_1												
6	22.5	45													
7	25.0	50													
8	27.5	55													
9	**30.0**	60		P_1											
10	32.5	65													
11	35.0	70													
12	37.5	75													
13	**40.0**	80			P_1										
14	42.5	85							P_1						
15	45.0	90				P_1		F_1		P_2		61	43	**ToS**	2 passes √
16	47.5	95					F_1				F_2	12	2	E	2 fails √
17	**50.0**	100												H	

4.4 ToS statistical analysis

To create baseline data for healthy young adults, it is important to understand what is normal. Normal ToS results can be identified by finding mean values and

determining the standard deviation. Watching for outliers, mean values for normal can be calculated. With sufficient baseline data, abnormalities in future tests can be more easily identified.

Recall that the ToS is a measure of the amount of stabilizing torque required to assist the participant during balancing. Thus, there are three factors that contribute to the subject's ToS; subject mass, height, and capability. Differences is subject mass and height were accounted for by developing a normalized distance (see equation 21 in the methods section). Linear regressions were used to verify that this normalization was necessary and that it was effective. The analysis will ultimately tell if normalization can be used to minimize the effect of subject mass and height in order to clearly measure subject balance capability.

P-values with a 95% confidence interval can be used to determine if a correlation exists between two parameters. A p-value less than .05 signifies that a significant correlation is present. An existing correlation indicates a trend that can be predicted and accounted for if properly managed.

4.4.1 Critical distance versus weight

A linear regression was performed to determine if the critical distance is correlated with participant weight. A fitted line plot was generated in Minitab, yielding a regression analysis with textual data and a visualization of the result. The p-value of 0.002 indicates that there is a correlation between these two parameters. As weight increased among the participants, their thresholds decreased correspondingly. A decrease in threshold indicated an increase in the critical distance of the spring from the center of the chair, $\boldsymbol{d_{crit}}$. These results show that weight is strongly correlated with the ToS. Therefore, normalization is needed in order to avoid confounding of the balance capability results by this factor. The results of critical distance versus height are shown in Figure 4.1.

Regression Analysis: d_crit (in) versus Weight (lbs)

The regression equation is

d_crit (in) = 2.704 + 0.01615 Weight (lbs)

Analysis of Variance

Source	DF	SS	MS	F	P
Regression	1	3.10033	3.10033	17.99	0.002
Error	10	1.72321	0.17232		
Total	11	4.82354			

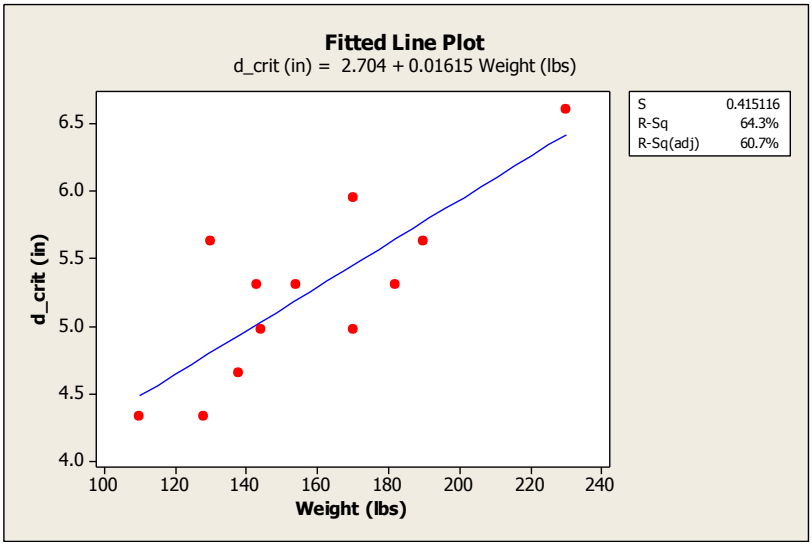

Figure 4.1: Graph of critical distance vs. weight.

4.4.2 Equilibrium distance versus weight

Equilibrium distance was a function of participant mass and critical distance, not performance. When compared with weight, the regression analysis yielded a p-value less than 0.05 at approximately 0.000. The fitted line plot appears to be extremely linear with very minimal deviation visible. There is a strong correlation between a participant's equilibrium distance and their weight. This result was expected because subject weight was used in the calculation of the equilibrium distance (see equation 17). The results of equilibrium distance versus weight are shown in Figure 4.2.

Regression Analysis: d_eq (in) versus Weight (lbs)

```
The regression equation is
d_eq (in) = 3.562 + 0.03574 Weight (lbs)
Analysis of Variance
Source       DF        SS        MS        F       P
Regression    1   15.1892   15.1892   272.07   0.000
Error        10    0.5583    0.0558
Total        11   15.7474
```

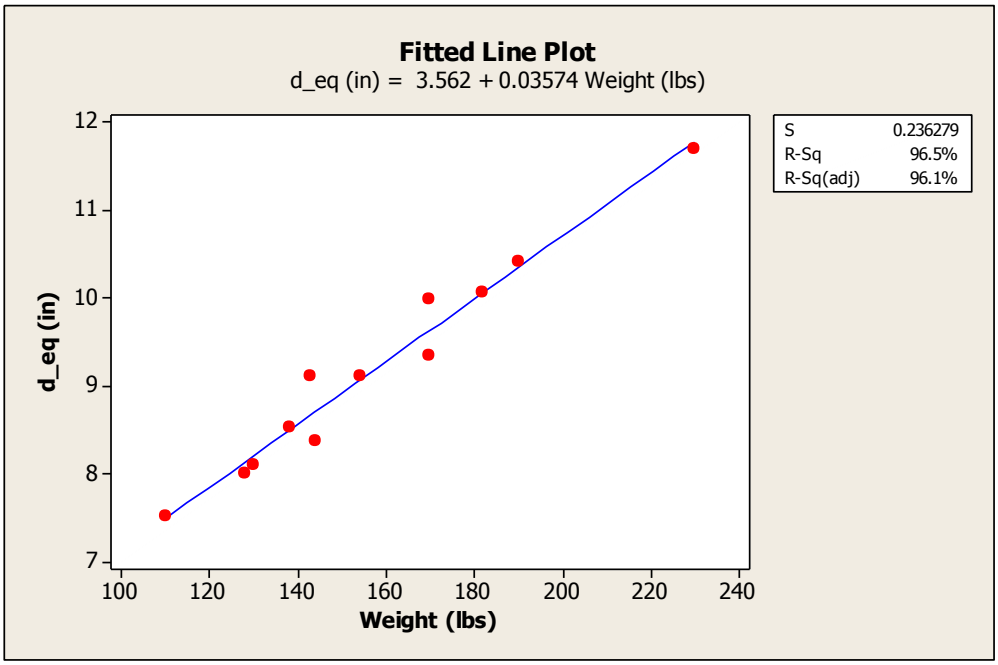

Figure 4.2: Graph of equilibrium distance vs. weight.

4.4.3 Normalized distance versus weight

Normalized distance was the final factor to be analyzed against weight. It was also the most pivotal because the intention of the normalization was to remove the correlation with subject height and weight in order to obtain a clear measure of the participant's ToS. When analyzed, the regression analysis produced a p-value of 0.370, exceeding the .05 threshold value. The change in p-value indicated that normalization was successful. The fitted line plot visually confirmed the success by revealing a highly random and non-linear sequence of points. The correlation had been removed, proving normalization was a success, as far as participant weight is concerned. The results of normalized distance versus weight are shown in Figure 4.3.

Regression Analysis: d_norm versus Weight (lbs)

```
The regression equation is
d_norm = 0.6445 - 0.000453 Weight (lbs)

Analysis of Variance
Source       DF         SS         MS      F      P
Regression    1  0.0024399  0.0024399   0.88  0.370
Error        10  0.0277156  0.0027716
Total        11  0.0301556
```

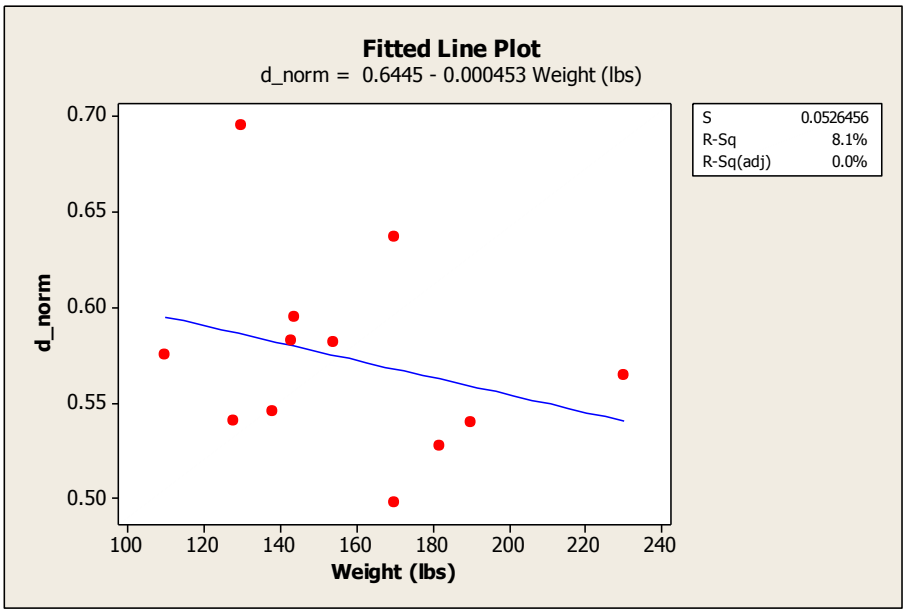

Figure 4.3: Graph of normalized distance vs. weight.

4.4.4 Critical distance versus height

Critical distance was the first of three height analyses. The regression analysis produced a p-value of 0.123, which although not significant raised some concern. Height was expected to influence the ToS, with taller the participants having greater values of d_{crit}. The fitted line plot appears somewhat random, but it does show a positive slope similar to weight. It is possible that the seating position altered participant height enough to somewhat normalize height. Alternatively, height may be a less important factor that weight when determining the ToS. The results of critical distance versus height are shown in Figure 4.4.

Regression Analysis: d_crit (in) versus Height (in)

```
The regression equation is
d_crit (in) = 0.743 + 0.06623 Height (in)

Analysis of Variance
Source       DF       SS       MS     F       P
Regression    1  1.06720  1.06720  2.84   0.123
Error        10  3.75635  0.37563
Total        11  4.82354
```

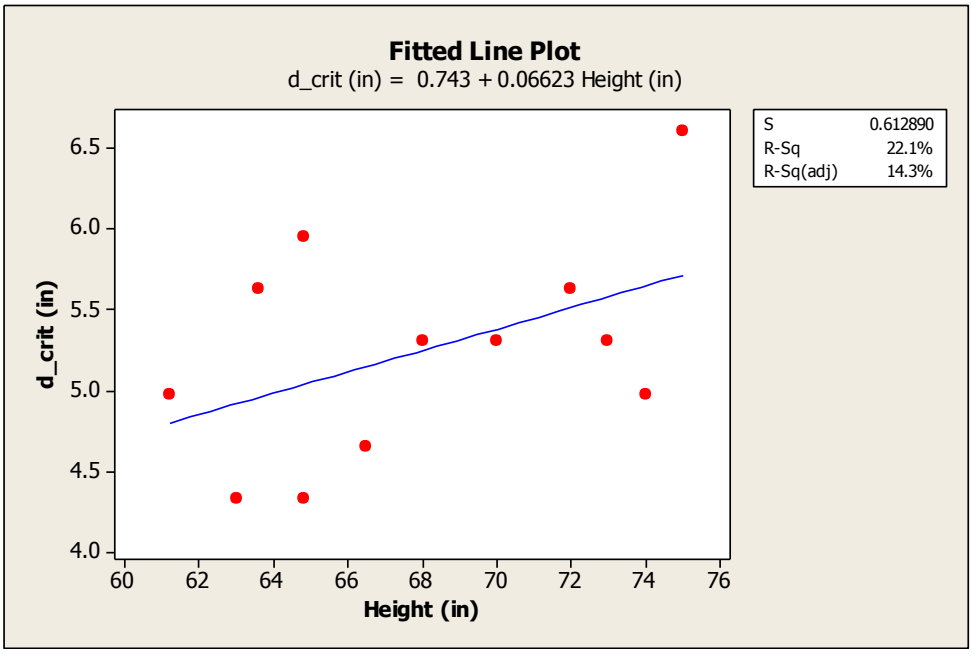

Figure 4.4: Graph of critical distance vs. height.

4.4.5 Equilibrium distance versus height

The equilibrium distance versus height had a significant positive correlation. The regression analysis produced a p-value of 0.001, similar to previous analyses for weight. Like the analysis of the equilibrium distance verses weight, these results were also expected because subject height was also used in the calculation of the equilibrium distance (see equation 17). The results of equilibrium distance versus height are shown in Figure 4.5.

Regression Analysis: d_eq (in) versus Height (in)

```
The regression equation is
d_eq (in) = - 4.999 + 0.2087 Height (in)

Analysis of Variance
Source       DF       SS       MS      F      P
Regression    1  10.5944  10.5944  20.56  0.001
Error        10   5.1531   0.5153
Total        11  15.7474
```

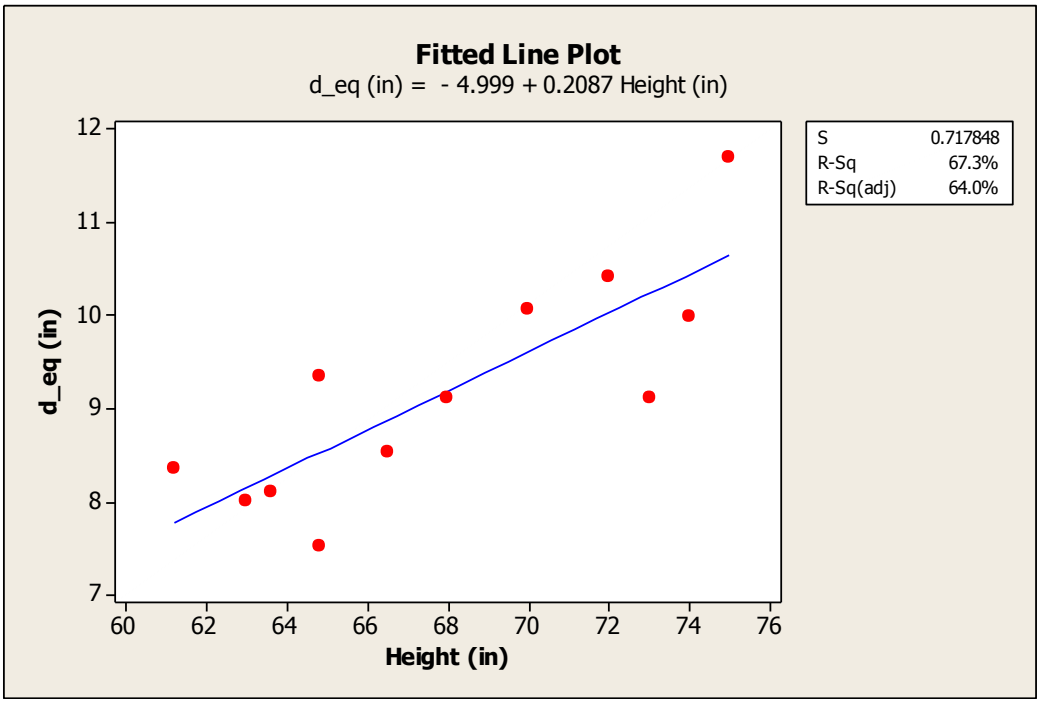

Figure 4.5: Graph of equilibrium distance vs. height.

4.4.6 Normalized distance versus height

The final regression analysis aims to further prove the validity of normalization. The derived p-value of 0.091exceeded 0.05 indicating that there was no significant correlation. The P-value is much closer to 0.05 than *normalized distance versus weight*, but the value still lies within a range that indicates the expected randomization that implies normalization worked. The low P-value may be attributed to the seating position of the kneeling chair. It is also interesting that the correlation was negative with height, possibly indicating an over compensation of this parameter. The results of normalized distance versus height are shown in Figure 4.6.

Regression Analysis: d_norm versus Height (in)

```
The regression equation is
d_norm = 0.9586 - 0.005668 Height (in)

Analysis of Variance
Source       DF         SS          MS      F      P
Regression    1  0.0078166  0.0078166  3.50  0.091
Error        10  0.0223389  0.0022339
Total        11  0.0301556
```

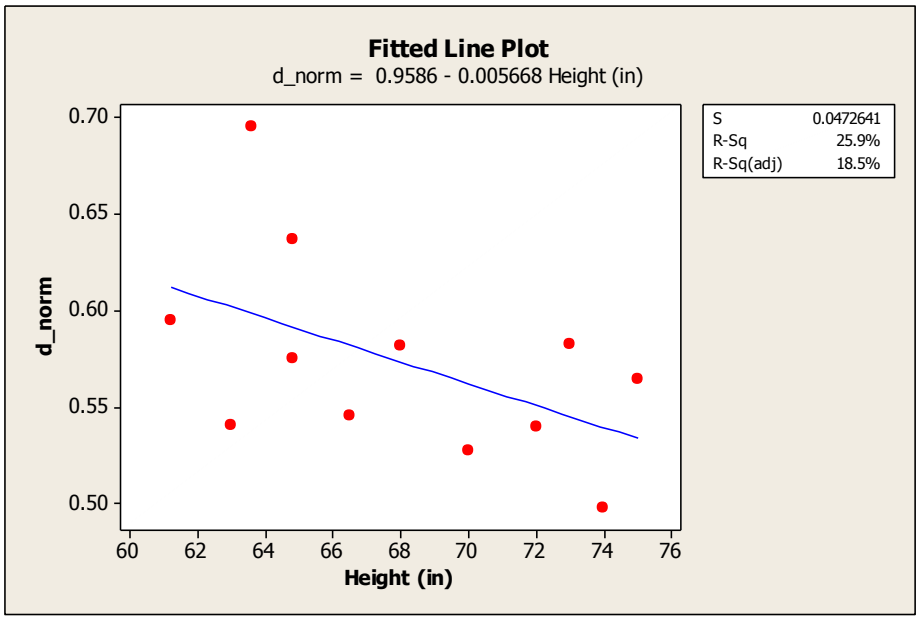

Figure 4.6: Graph of normalized distance vs. height.

4.4.7 Gender versus critical distance

Further analysis of the ToS results were performed with two sample t-tests. Three tests were run, to determine if there was a difference in the ToS capabilities between male and female subjects. The data was tested for equal variances (Levene's test) in order to determine if equal variance should be assumed in the t-test calculation. The null hypothesis was that the population variances are equal. The test for equal variance was applied to the critical distance and found to be not significant (p=0.702). This means that the t-test should be performed using equal variances. The T-test yielded a p-value of 0.166, failing to reject the null hypothesis. The female mean for critical distance was found to be equal to the male mean. Thus according to this parameter, there is no difference in balance capability between males and females.

Null hypothesis (H0): $\mu_A = \mu_B$ (Female has equal mean to Male)

Test and CI for Two Variances: d_crit (in) vs Gender

```
Gender  N  StDev  Variance
F       6  0.682     0.465
M       6  0.569     0.324
Ratio of standard deviations = 1.198
Ratio of variances = 1.435

95% Confidence Intervals
                                   CI for
Distribution   CI for StDev       Variance
of Data            Ratio           Ratio
Normal        (0.448, 3.202)  (0.201, 10.254)
Continuous    (0.437,     *)  (0.191,      *)
                                          Test
Method                          DF1  DF2  Statistic  P-Value
F Test (normal)                   5    5       1.43    0.702
```

Two-Sample T-Test and CI: d_crit (in), Gender

```
Two-sample T for d_crit (in)
Gender  N   Mean  StDev  SE Mean
F       6  4.975  0.682     0.28
M       6  5.517  0.569     0.23

Difference = mu (F) - mu (M)
Estimate for difference:  -0.542
95% CI for difference:  (-1.349, 0.266)
T-Test of difference = 0 (vs not =): T-Value = -1.49  P-Value = 0.166  DF
= 10
```

4.4.8 Gender versus equilibrium distance

Equilibrium distance also acquired a not significant p-value of 0.349 when tested for equal variances. The t-test produced a p-value of 0.004. As a result, the null hypothesis was rejected. Equilibrium distance was found to be dependent upon gender with the mean value for males (10.064") being significantly greater than that of females (8.312"). This result was expected and indicates that the males in the study group and were larger (mass and height) than the females. Equilibrium distance does not measure performance, only height and weight. Males were significantly heavier as quantified by d_{eq}.

Alternative hypothesis (H1): $\mu_A \neq \mu_B$ (Female mean is not equal to Male)

Test and CI for Two Variances: d_eq (in) vs Gender

```
Statistics
Gender  N  StDev  Variance
F       6  0.616     0.379
M       6  0.963     0.927

Ratio of standard deviations = 0.640
Ratio of variances = 0.409

95% Confidence Intervals
                                    CI for
Distribution   CI for StDev       Variance
of Data            Ratio           Ratio
Normal        (0.239, 1.711)  (0.057,  2.926)
Continuous    (0.108, 5.565)  (0.012, 30.972)

Tests
                                          Test
Method                          DF1  DF2  Statistic  P-Value
F Test (normal)                   5    5       0.41    0.349
```

Two-Sample T-Test and CI: d_eq (in), Gender

```
Gender  N    Mean  StDev  SE Mean
F       6   8.312  0.616     0.25
M       6  10.064  0.963     0.39

Difference = mu (F) - mu (M)
Estimate for difference:  -1.753
95% CI for difference:  (-2.792, -0.713)
T-Test of difference = 0 (vs not =): T-Value = -3.76  P-Value = 0.004  DF
= 10
Both use Pooled StDev = 0.8081
```

4.4.9 Gender versus normalized distance

The final test was for normalized distance. The p-value for the test for equal variance was 0.236, so the variances were again equal. The t-test produced a p-value of 0.107. The test failed to reject the null hypothesis indicating that there was no difference in balance capability between genders.

Null hypothesis (H0): $\mu_A = \mu_B$ (Female has equal mean to Male)

Test and CI for Two Variances: d_norm vs Gender

```
Gender  N  StDev  Variance
F       6  0.059     0.003
M       6  0.033     0.001
Ratio of standard deviations = 1.770
Ratio of variances = 3.133

95% Confidence Intervals
                                    CI for
Distribution   CI for StDev       Variance
of Data            Ratio           Ratio
Normal        (0.662, 4.732)  (0.438, 22.393)
Continuous    (0.387, 4.063)  (0.150, 16.511)

Tests
                                          Test
Method                          DF1  DF2  Statistic  P-Value
F Test (normal)                   5    5       3.13    0.236
```

Two-Sample T-Test and CI: d_norm, Gender

```
Two-sample T for d_norm
Gender  N    Mean   StDev  SE Mean
F       6  0.5977  0.0590    0.024
M       6  0.5488  0.0333    0.014

Difference = mu (F) - mu (M)
Estimate for difference:  0.0489
95% CI for difference:  (-0.0127, 0.1106)
T-Test of difference = 0 (vs not =): T-Value = 1.77  P-Value = 0.107  DF
= 10
Both use Pooled StDev = 0.0479
```

4.5 Basin of Stability results

The BoS data was collected to obtain preliminary data on the performance of the BoS chair. Each participant was tested at two difficulty levels (easy and hard). Of the twelve participants tested, a majority yield optimal results. Those trials were optimal because the participants involved had fallen at least four times in one data set. Two participants did not achieve four falls on their easy difficulty, and further trials were terminated after four attempts. Two female participants were not able to finish the BoS testing. Participant number 3 reached the maximum capability of the BoS chair, and could not progress any further to the BoS testing. Participant number 3 achieved a d_{norm} value of 54%, which was statistically the third highest in ToS performance (Participant 7 at 50%, Participant 11 at 53%). Therefore, her balance skill was regarded above average, but not the best of the group. Her small mass combined with her above average balance skill lead her to achieving a ToS of 100%.

Participant number 6 performed closely to participant number 3. Though her performance was similar, it was still possible to test an easy difficulty because her threshold was low enough. Participant number 6 was the smallest subject in terms of mass, and her d_{norm} value was 58%. She tended to show less balance skill, so her low mass played a bigger role in achieving a high ToS.

A new data set was created and exported to an individual text file for every trial. The data sets were recorded in numerical point cloud form consisting of the coordinates detected by the sensor. Data was collected at 100 Hz, offering a high level of detail. The X-axis indicated medial-lateral movement and was dubbed “Roll,” and the Y-axis indicated anterior-posterior movement and was dubbed “Pitch.”

Roll and Pitch values were represented as the numeric angle offset from zero (0.0), the upright vertical position. Zero was the point at which the sensor was completely level on a given axis, based on the gravitational pull on the sensor itself. The chair was previously adjusted to be completely level at rest and the sensor was zeroed prior to beginning each test. The Z-axis (twisting motion) was available in the data set, but not used.

4.5.1 Stability graph

The stability graph displayed the angle of the base during the BoS trial over a two minute period (120 seconds). The X and Y axes were recorded, imported into a spreadsheet, and graphed (Figure 4.7). The roll values (blue) represented frontal plane (side to side) motion. The pitch values (red) represented sagittal plane (forward and aft) motion. Stable motion was observed as erratic movement near the zero value. Falls are observed as large perturbations that extend far beyond the average magnitude of oscillation. The chart above displays a participant that fell forward four times and then fell to the back one time. No lateral falls occurred in this data set as indicated by minimal deviation of the roll parameter. This data was considered ideal because multiple falls were detected, yet stable motion was still seen between each fall.

Table 4.4: Motion sensor raw data.

Time (s)	Roll	Pitch	Roll Abs	Pitch Abs	Roll Velocity	Pitch Velocity
0	1.147169	6.359974	1.147169	6.359974	--	--
0.01	1.005828	6.34512	1.005828	6.34512	-14.1341	0.105093356
0.02	0.882891	6.333261	0.882891	6.333261	-12.2937	0.096464043
0.03	0.771866	6.329954	0.771866	6.329954	-11.1025	0.029786084
0.04	0.681212	6.33192	0.681212	6.33192	-9.0654	-0.021686853
0.05	0.599701	6.341254	0.599701	6.341254	-8.1511	-0.114512152
…	…	…	…	…	…	…

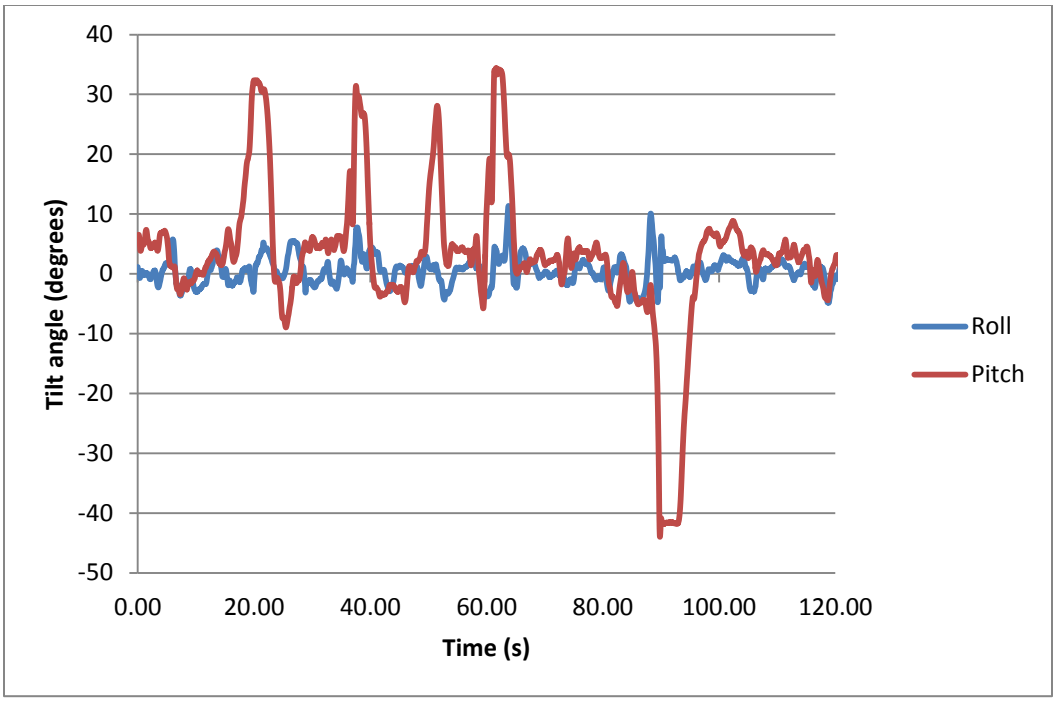

Figure 4.7: Stability graph representing two axes of motion used for dividing the sagittal and coronal planes.

4.5.2 Stabilogram

The stabilogram is a graphical representation of kinematic variability. It traces the trajectory of the movement in two dimensions. The result may be equated to a "birds-eye-view" of the path that a participant followed throughout the trial. It is more difficult to identify falls in the stabilogram, but it does reveal the true direction of each fall. The stabilogram above represents a participant that remained mostly stable, with a few falls forward, and two falls to the rear. One limitation of the stabilogram is that it does not provide the path direction so one cannot tell from visual observation which curve is approaching and which is leaving equilibrium. The stabilograms generated were used only to verify that the data was valid will be used in future work to measure the BoS

using this device. Figure 4.8 is an example of one of the stabilograms generated for baseline data.

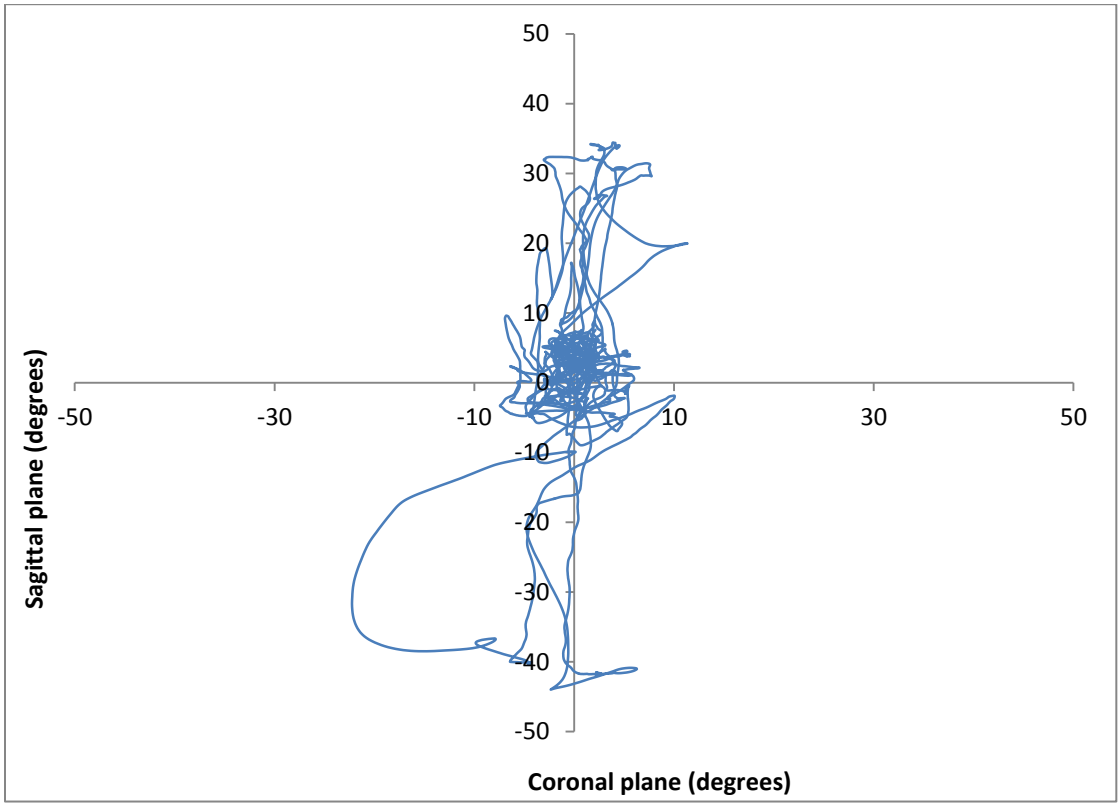

Figure 4.8: Stabilogram representing kinematic variability.

4.6 Basin of Stability analysis

The Basin of Stability test results were compiled into two spreadsheets, dividing the data into easy and hard modes. It required multiple trials for some participants to gather sufficient data. Each trial was categorized in terms of the cumulative number of seconds required to gather sufficient data (120, 240, 360). In each trial column, the number of falls was recorded. The total number of falls was summed together, as well as the total trial time. Total falls were divided by total time (in minutes) to produce the

number of falls per minute. Falls per minute simplified the partitioned trials into one value for statistical analysis.

Table 4.5: Compiled BoS results with easy modes (top), and hard modes (bottom).

Participant	ToS	Tested	120s	240s	360s	Total Falls	Total Time (s)	Falls per minute
1	80%	85%	3	5		8	240	2.00
2	80%	85%	2	1	1	4	360	0.67
3	100%							
4	75%	80%	2	3		5	240	1.25
5	85%	90%	6			6	120	3.00
6	95%	100%	5			5	120	2.50
7	85%	90%	5			5	120	2.50
8	70%	75%	2	2		4	240	1.00
9	90%	95%	5			5	120	2.50
10	75%	80%	3	2		5	240	1.25
11	80%	85%	5			5	120	2.50
12	60%	65%	4			4	120	2.00
Participant	**ToS**	**Tested**	**120s**	**240s**	**360s**	**Total Falls**	**Total Time (s)**	**Falls per minute**
1	80%	95%	5			5	120	2.50
2	80%	95%	5			5	120	2.50
3	100%							
4	75%	90%	3			3	120	1.50
5	85%	100%	2	4		6	240	1.50
6	95%		2	2		4	240	1.00
7	85%	100%	4			4	120	2.00
8	70%	85%	5			5	120	2.50
9	90%	100%	5			5	120	2.50
10	75%	90%	2	4		6	240	1.50
11	80%	95%	8			8	120	4.00
12	60%	75%	6			6	120	3.00

BoS performance was statistically analyzed to determine if differences could be found between easy and hard difficulties. Similar to the analysis of the ToS, a test for equal variances was performed and found to be $p = 0.750$. Thus, a two-sample t-test was

performed, assuming equal variances. No significant differences were found between the easy and hard difficulties (p=0.389).

Null hypothesis (H0): $\mu_A = \mu_B$ (Easy has equal mean to Hard)

Alternative hypothesis (H1): $\mu_A \neq \mu_B$ (Easy mean is not equal to Hard)

Test and CI for Two Variances: Falls per minute vs Difficulty

```
Statistics

Difficulty   N  StDev  Variance
E           11  0.764     0.584
H           11  0.847     0.718

Ratio of standard deviations = 0.902
Ratio of variances = 0.813

95% Confidence Intervals
                                 CI for
Distribution   CI for StDev      Variance
of Data            Ratio           Ratio
Normal        (0.468, 1.738)  (0.219, 3.022)
Continuous    (0.473, 2.994)  (0.223, 8.965)
                                          Test
Method                          DF1  DF2  Statistic  P-Value
F Test (normal)                  10   10       0.81    0.750
```

Two-Sample T-Test and CI: Falls per minute, Difficulty

```
Two-sample T for Falls per minute

Difficulty   N   Mean  StDev  SE Mean
E           11  1.924  0.764     0.23
H           11  2.227  0.847     0.26

Difference = mu (E) - mu (H)
Estimate for difference:  -0.303
95% CI for difference:  (-1.021, 0.415)
T-Test of difference = 0 (vs not =): T-Value = -0.88  P-Value = 0.389  DF = 20
Both use Pooled StDev = 0.8069
```

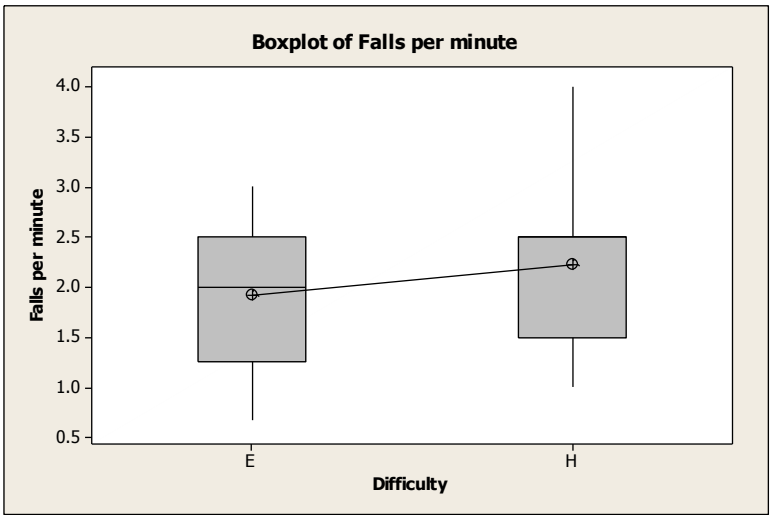

Figure 4.9: Boxplot of falls per minute for visual comparison.

Null hypothesis (H0): $\mu_A = \mu_B$ (Easy has equal mean to Hard)

This analysis observes only the number of falls over time. The easy and hard modes were both set close to the participant threshold to ensure that participants would exhibit their balance control at a region that is unstable but balance can be maintained for a number of seconds. The two modes were statistically found to be similar, indicating that they are both within the desired range.

CHAPTER 5: DISCUSSION

5.1 Basin of Stability chair development

The methods used during design and fabrication were mostly successful. The choice to buy the pre-determined compression springs and pivot joint parts ahead of the design helped move the process along. It proved to be essential to have tangible parts to work with in the design phase, to ensure design followed function. The fabrication of repeated parts across one piece of material, before cutting them into each respective piece, saved hours of work. The process also ensured that such parts were identical, while reducing machining setup times by 90% (if 16 parts are yielded from one piece of stock). Other less methodical processes included the design of sliders and friction areas, which required trial and error. It took several iterations to find that PVC was a suitable material for the spring enclosure sliders, but the end result was a smooth and quiet functioning device.

The BoS chair met the design objectives of achieving large angular deflections, adjustable difficulty, and the ability to stabilize and destabilize a test subject. Despite a few reports of discomfort at the knee pads, no injuries were sustained among all participants. This can be attributed to an appropriately designed device, test protocol and safety frame. The BoS chair structure proved to be durable and reliable. The main supporting column remained rigid throughout testing, and is suitable for future work.

The completed device collected valid Threshold of Stability information, and preliminary Basin of Stability data. All participants were tested with increasing difficulty which led to an eventual loss of stability. Though participants tried not to fall, and

believed they were not supposed to, there were multiple reports indicating that the experience was enjoyable. The consensus was that the chair was somewhat comfortable, though it was reported to cause some knee irritation. The geometry was suitable for accommodating varying sizes of participants. The safety frame was considered a bit daunting for most participants, but after their first practice fall, they admitted it was not as scary as they had thought. The process of mounting the chair proved awkward for every participant. This awkwardness was minimized by having each participant would watch the researcher demonstration the mounting process. In addition, participants were assisted with the mounting process but the research staff. A simplified mounting process is ideal in eliminating many of the hurdles that come before testing. Some participants were relieved to end testing, but other wanted to continue trying after the testing was completed. Overall, the BoS chair was awkward at first, but for many, it was comfortable and enjoyable.

5.2 Study Limitations and Unexpected Discoveries

Throughout the BoS research, a few mistakes were made and problems with the test protocol were discovered. For instance, confusion sometimes arose during a trial and the progressively changing difficulty settings were not changed correctly. During testing it was discovered that some participants were too light to perform at higher difficulties on the BoS chair. This was found to be a limitation of the device which can be corrected by changing the springs to ones with a lower spring constant. Although an approximate spring constant was calculated analytically, the ideal spring constant could not be determined until the device was built and tested. The upright seated position of the

kneeling chair posed issues with the testing procedure. From the beginning, iIt was known that the upright position was not optimal because of the large distance between the center of mass and the pivot point.. The optimal position would place the participant's pelvis region at the pivot point, isolating the upper and lower torsos. Such a position would require the gimbal design, placing the moving components of the BoS chair around the participant. The design would be much more elaborate, and possibly require four times the amount of floor space. Ultimately, the BoS chair's true and final design was chosen for its overall feasibility.

The Basin of Stability tests yielded only one concerning finding. Some participants showed signs of performing differently than their ToS trials. Where a participant may have fallen within 60 seconds multiple times at one specific difficulty during the ToS trials, they did not always fall within the two minute BoS trials of that difficulty. Participants were intentionally not provided with too much detailed about the purpose of the tests and just told to "try your best". The participants were simply instructed on what to do, and when.

5.3 Significant findings

Six regression analyses were run regarding the ToS results. The analyses were used to indicate the correlations between weight or height to critical distance, equilibrium distance, and normalized distance. It was expected that height and weight would both have direct correlations with critical distance and equilibrium distance. Additionally, it was expected that normalization with height and weight would remove those correlations. The six analyses did support the theory except for one irregularity. Height and critical distance were not found to be significantly correlated, as in the previous Figure 4.4. The

lack of correlation was likely attributed to the offset height of the kneeling chair, in conjunction with the kneeling posture of the participant. The height versus critical distance graph did appear to show some positive correlation however. From the analysis, it can be assumed that height did have effect on the critical distance.

Normalization proved to be necessary and effective. Prior to normalization the performance parameter d_{crit} was found to be correlated with weight and trended toward a correlation with height. However after normalization, not correlation was observed with either height or weight.

Table 5.1: Summary of the ToS analysis of height and weight. †trend observed

weight vs. d_{crit} = correlation	*height vs.* d_{crit} = no correlation†
weight vs. d_{eq} = correlation	*height vs.* d_{eq} = correlation
weight vs. d_{norm} = no correlation	*height vs.* d_{norm} = no correlation

The ToS results were reordered in ascending order of best normalized performance (d_{norm}) to worst. The largest participant (by mass) was 6^{th} indicating that this persons balance skill is close to the median value. However, without normalization, the raw results indicated that subject 12 did very poorly with a d_{crit} of 6.60. This further shows that normalization was a necessary and successful. A proven normalization method is useful because it assists in faster analysis and provides insight on finding a way to pre-normalize tests by adjusting spring rates per participant.

Table 5.2: ToS results in ascending order of $d_{norm.}$

Subject	Gender	Age (yrs)	Weight (lbs)	Height (in)	ToS (Cp)	d_comp (in)	d_crit (in)	d_eq (in)	d_norm
7	M	24	170	74.0	85%	5.53	4.98	9.99	49.8%
11	M	24	182	70.0	80%	5.20	5.30	10.06	52.7%
4	M	22	190	72.0	75%	4.88	5.63	10.42	54.0%
3	F	23	128	63.0	95%	6.18	4.33	8.00	54.1%
9	F	28	138	66.5	90%	5.85	4.65	8.53	54.5%
12	M	24	230	75.0	60%	3.90	6.60	11.70	56.4%
6	F	30	110	64.8	95%	6.18	4.33	7.52	57.5%
1	M	24	154	68.0	80%	5.20	5.30	9.12	58.1%
2	M	24	143	73.0	80%	5.20	5.30	9.10	58.2%
5	F	22	144	61.2	85%	5.53	4.98	8.36	59.5%
8	F	20	170	64.8	70%	4.55	5.95	9.35	63.6%
10	F	20	130	63.6	75%	4.88	5.63	8.10	69.4%

CHAPTER 6: CONCLUSION

The scope of this project included the design, construction and testing of a novel device used to measure torso stability over large angular deflections, the BoS chair. In addition, the device was used to measure the ToS and BoS in 12 subjects to obtain baseline values for normal healthy subjects using this device. This study using the BoS chair showed that torso balance control capability of healthy young participants could be evaluated, regardless of their size. The stability graphs and stabilograms generated from the preliminary BoS data indicated that the recording device and trial methods were sufficient. These initial Basin of Stability tests will form the foundation for the development of future BoS testing protocols.

The BoS chair is as a durable and flexible tool for measuring torso stability that was designed to detect Lagrangian Coherent structures like no other device in the world. The preliminary BoS data collected in this research will be useful for future Basin of Stability research and provide preliminary data for grant proposals. With the device constructed and baseline data available for normal human subjects (i.e. controls), we are now prepared for future projects that measure torso stability in patient populations to improve our understanding of this condition and its effect on low back pain.

6.1 Recommendations and Future Work

The design of the BoS chair is versatile enough for numerous modifications and has attachment points for new sensors and features. Future work includes maintenance and design optimizations to enhance hair performance. Details are provided in the

paragraphs below. Device maintenance may be required if future testing is extensive. The BoS chair may be meticulously examined for part wear and reworking performed. Potential areas include joints, connections and bearings that could be subject to failure.

A large number of the participants were very light. These smaller participants nearly reached the maximum difficulty of the chair with little effort. Larger participants showed no signs of having difficulty balancing at the lower difficulties. Such observations implied that the difficulties were too “easy” and that the springs were too strong. This lead to all tested participants bypassing the lower 40% difficulty region. It will be necessary for future work to adjust the difficulty levels of the chair. The difficulties must be shifted in favor of having higher difficulties, truncating the lower difficulties. The simplest way to make the adjustment would be to replace the DWC-281R-23 springs to achieve a lower spring rate. If possible, it would be ideal to replace the original springs with ones of similar dimensions to avoid alteration of the spring enclosures. The result of the spring replacement should remove approximately 25% of the lower difficulties, to achieve 25% more of the higher difficulties.

Based on participant feedback, the chair design was somewhat comfortable in terms of the geometric proportions. However, some participants reported that the knee rest caused some irritation. Extra knee padding was offered to these participants. The issue might be attributed to excessive pressure of the knee upon a flat, lightly padded surface. The recommended solution, based upon observations, is to add ergonomic enhancements to the entire chair. The next iteration of the chair could include grooves shaped to general body dimensions in the contact areas to distribute pressure and influence proper sitting positions. Enhanced or thicker foam for the knee rest is also

recommended. The steel cables used to connect the springs to the upper pivot plate are among many parts subject to wear. The cables, however, are the most critical item to maintain. The loss of one cable would destabilize the chair and could send a participant falling abruptly to one side. Though the safety frame exists for such occurrences, a broken cable could be startling for the participant. It is highly recommended that the cables be inspected for frays, loose crimp connections or rubbing areas before each trial. The cables did not show signs of wear following this study.

Bibliography

Blaszczyk, J. W. (2008). Sway ratio - a new measure for quantifying postural stability. *Acta Neurobiologiae Experimentalis, 68*(1), 51-57.

Bogduk, N., & Twomey, L. T. (2009). *Clinical and radiological anatomy of the lumbar spine* (5th edition ed.). Melbourne: Churchill Livingstone.

Dickey, J. P., Pierrynowski, M. R., Galea, V., Bednar, D. A., & Yang, S. X. (2000). Relationship between pain and intersegmental spinal motion characteristics in low-back pain subjects. *Systems, Man, and Cybernetics, 2000 IEEE International Conference on, , 1.* pp. 260-264 vol.1.

Dieen JHV, Cholewicki J, Radebold A. Trunk muscle recruitment patterns in patients with low back pain enhance the stability of the lumbar spine. Spine 2003;28(8):834-41. [PubMed: 12698129]

Frank, J. W., Kerr, M. S., Brooker, A. S., DeMaio, S. E., Maetzel, A., Shannon, H. S., et al. (1996). Disability resulting from occupational low back pain. part I: What do we know about primary prevention? A review of the scientific evidence on prevention before disability begins. *Spine, 21*(24), 2908-2917.

Lv Jiefeng. (2009). To adapt, to guide and to interact —three models of human-product relationship. *Computer-Aided Industrial Design & Conceptual Design, 2009. CAID & CD 2009. IEEE 10th International Conference on,* pp. 168-171.

Marras, W. S., Parnianpour, M., Kim, J. -. Y., Ferguson, S. A., Crowell, R. R., & Simon, S. R. (1994). The effect of task asymmetry, age and gender on dynamic trunk motion characteristics during repetitive trunk flexion and extension in a large normal population. *Rehabilitation Engineering, IEEE Transactions on, 2*(3), 137-146.

Panjabi MM. Clinical spinal instability and low back pain. Journal of Electromyography and kinesiology 2003;13(4):371-379. [PubMed: 12832167]

Panjabi, M.M., *The stabilizing system of the spine. Part I. Function, dysfunction, adaptation, and enhancement.* J Spinal Disord, 1992. **5**(4): p. 383-9

Panjabi, M.M., *The stabilizing system of the spine. Part II. Neutral zone and instability hypothesis.* J Spinal Disord, 1992. **5**(4): p. 390-6

Radebold, A., Cholewicki, J., Polzhofer, G. K., & Greene, H. S. (2001). Impaired postural control of the lumbar spine is associated with delayed muscle response times in patients with chronic idiopathic low back pain. *Spine, 26*(7), 724-730.

Ransford, A. O, Cairns, D., Mooney, V. (1976 "The Pain Drawing as an Aid to Psychologic evaluation of Patients with Low-Back pain", Spine, 1 (2), 127-134.

Reeves, N. P., & Cholewicki, J. (2003). Modeling the human lumbar spine for assessing spinal loads, stability, and risk of injury. *Critical Reviews in Biomedical Engineering, 31*(1-2), 73-139.

Ross, S. D., Tanaka, M. L., & Senatore, C. (2010). Detecting dynamical boundaries from kinematic data in biomechanics. *Chaos: An Interdisciplinary Journal of Nonlinear Science,20*(1), 017507.

Ruhe, A., Fejer, R., & Walker, B. (2011). Center of pressure excursion as a measure of balance performance in patients with non-specific low back pain compared to healthy controls: A systematic review of the literature. *European Spine Journal : Official Publication of the European Spine Society, the European Spinal Deformity Society, and the European Section of the Cervical Spine Research Society, 20*(3), 358-368.

Ruhe, A., Fejer, R., & Walker, B. (2011). Is there a relationship between pain intensity and postural sway in patients with non-specific low back pain? *BMC Musculoskeletal Disorders, 12*, 162.

Spyridonis, F., & Ghinea, G. (2010). A pilot study to examine the relationship of 3D pain drawings with objective measures in mobility impaired people suffering from low back-pain. *Engineering in Medicine and Biology Society (EMBC), 2010 Annual International Conference of the IEEE,* pp. 3895-3898.

Tajali, S., Negahban, H., Yazdi, M. J. S., Salehi, R., Mehravar, M., & Parnianpour, M. (2011). The effects of postural difficulty conditions on variability of joint kinematic patterns during sit to stand task in normals and patients with non-specific chronic low back pain. *Biomedical Engineering (MECBME), 2011 1st Middle East Conference on,* pp. 300-303.

Tanaka, M. L., Nussbaum, M. A., & Ross, S. D. (2009). Evaluation of the threshold of stability for the human spine. *Journal of Biomechanics, 42*(8), 1017-1022.

Tanaka, M. L., Ross, S. D., & Nussbaum, M. A. (2010). Mathematical modeling and simulation of seated stability. *Journal of Biomechanics, 43*(5), 906-912.

Vaughn, M. L., Cavill, S. J., Taylor, S. J., Foy, M. A., & Fogg, A. J. B. (1999). Using direct explanations to validate a multi-layer perceptron network that classifies low back pain patients. *Neural Information Processing, 1999. Proceedings. ICONIP '99. 6th International Conference on, , 2.* pp. 692-699 vol.2.